UNIVERSITY OF TARTU
INSTITUTE OF ECOLOGY AND EARTH SCIENCES
DEPARTMENT OF GEOLOGY

Jekaterina Nezdoli

Study of inorganic component within the Meenikunno bog (SE Estonia) peat

Master thesis (30 EAP)

Supervisor: Jüri Plado

Tartu 2015

Table of contents

1. Introduction

In this master thesis the author reports on ground-penetrating radar (GPR) studies of Meenikunno bog, its stratigraphy based on drillings, and the description of the non-organic component found in peat. The non-organic component is studied by the means of magnetic susceptibility, loss on ignition, binocular and light microscopes, and geochemical methods such as SEM-EDS and ICP-MS. The results are compared with the Meenikunno mineral grains from Mrs. Reet Tiirmaa collection (1999). This is aimed to find, describe, and hint for the origin of non-organic component within the Meenikunno peat.

The study was initiated by an article (Raukas et al., 2001) where extraterrestrial spherules were reported while studying non-organic material from Meenikunno bog peat. There, the findings were tied with near-by Ilumetsa structures. The study, however, didn't illustrate the findings nor studied their chemical composition, essential to prove the impact origin (e.g., French and Koeberl, 2010).

The Earth`s surface is surely capable of preserving traces of geological events such as impacts of extraterrestrial bodies. However, the geological processes are dynamic, and as the time passes, the significant changes occur. These changes make it harder to recognize and prove impact events. One of the ways to do that is to find the possibly preserved material.

An extraterrestrial object striking Earth at cosmic velocity melts and vaporizes silicate material, which can condense into highly spheroidal, sand-size particles. These particles known as impact spherules have been detected in great abundance in thin, discrete layers (Simonson & Glass, 2004). The spherules can travel several hundreds of km suspended in air from various sources. In case of impact structures, their spatial distribution is divided into proximal and distal ejectas (Niyogi *et al*., 2011). Any ejecta deposited >5 crater radii from the rim of the crater is considered distal (Simonson & Glass, 2004).

There is a place for natural preservation of spherules from the impacts of Holocene age: peatlands. Not only can they preserve distal evidence from impact, but also provide possibilities for the estimation of the exact time of the event.

2. Background

2.1. Use of peatlands in event stratigraphy

Peat growth is dependent on climatic conditions, and in different climatic periods it has not been uniform. The peat growth rate may vary considerably in different regions and even between individual parts of the same mire. According to Ilomets (1994), Estonian peat fens have an annual growth on average 0.5 mm / year, whereas bogs show faster rate: 1.5 mm / year. In total, Estonian marshes produce from 0.92 to 1.42 mln tons of peat annually. Because of on-going decomposition and compaction within a peat deposit, depth generally is not linearly related to age (Clymo et al., 1990).

The amount of mineral component (ash content) in peat depends on the way of nutrition during the formation of mire. In its fen or transitional stage, content of mineral component of 5-15 % is observed (Kink et al., 1998), whereas mineral particles are carried in by either ground or surface water. The mineral content in bog stage is as low as 1-3 % as inorganic material travels there mostly via precipitation and wind.

Earth`s atmosphere is known (Perle, 2014) to contain volatile material of various composition and origin. It tends to settle down on Earth`s surface and form a correspondent layer. The layer can be later used as a stratigraphic marker to determine sediments` age and geological events that happened in the past. This method is widely used in peatland studies as they provide excellent environment for preservation of such material (Perle, 2014). Furthermore, peat layers are easy to date by ^{14}C method (except last 100 years). There exist three common markers within peat: (i) fly-ash particles from the burning of fossil fuels, (ii) tephra (volcanic ash) produced by volcanic eruptions, and (iii) microtektites (glassy spherules) that are formed along with meteorite impact events.

In Estonia, the research on fly-ash particles by Marini & Raukas (2009) showed that studies on cosmic- and impact-related micro- spherules may seriously be hampered by outcrop- and laboratory contamination. Fly-ash particles and steel slags resembling iron-rich cosmic spheres are the most frequently invoked industrial contaminants. In contrast, little attention has been paid to glassy spherules of industrial origin that might resemble microtektites.

Hang et al. (2006) reported the first discovery of middle Holocene cryptotephra from a Mustjärve peat sequence in Estonia. Colourless tephra shards were identified at 312-316 cm.

Electron microprobe analyses suggest a correlation with the initial phase of the Hekla-4 eruption (4260 cal. yr BP). The low concentration and small size of the tephra particles indicate that Estonian bogs are probably on the verge of where tephrochronology is possible in north-western Europe. Further studies of full Holocene sequences are required in order to discover traces of other ash plumes reaching as far east as the eastern Baltic area.

The most of Estonian research, however, was done on glassy spherules in relation to meteoritic impact. For example, Kaali meteor crater and its surrounding peatlands were extensively studied (Raukas et al., 2000a, b; 2011; Veski et al., 2001; Moora et al., 2012; Perle, 2014).

2.2. Meenikunno bog

Meenikunno ombrotrophic bog is located in SE of Estonia, in the southern part of the Ugandi Plateau (Fig. 1). The closest populated point is Veriora village that is located 6 km NE of Meenikunno peatland. Its SW part was formed by the terrestrialization of a water body, in other parts the bog peat lies on a sandy soil. The Meenikunno Reserve embraces two Nohipalu lakes, Valgejärv, and Mustjärv. These lakes are connected with the bog and get their water from it. Meenikunno bog has 19 mineral "islands" and ridges buried under its peat (Masing et al., 1997).

The eastern part of the deposit refers to Meenikunno Nature Reserve since 1981. The western part of Meenikunno peat deposit was studied by geologists from Keila geological expedition in 1984-1985. They conducted a peat drill coring technique to estimate the thickness of peat deposit. The areal density of coring was 100 × 100 m, and the thickness of peat was identified with the accuracy of 0.1 m (Salo et al., 1985).

According to the investigation of Salo et al. (1985), the maximal thickness of Meenikunno peat deposit is 7.1 m, whereas its mean thickness is 2.7 m. Inferred from the occasional occurrence of 0.25 m thick sapropel layer under the peat, paludification of the area began 7600±80 years ago (C^{14} method; absolute age based on peat from a depth of 6.2 - 6.3 m) as a result of lake`s terrestrialization. Peat layers are mostly of bog type, but transitional mire is

Figure 1. Digital terrain model of the Meenikunno bog. The base for a model was obtained from Estonian Land Board (X-GIS). Red arrows indicate the two craters of Ilumetsa site: Põrguhaud and Sügavhaud.

also present. First, mesotrophic plants were decomposed to form transitional mire. Later, after the rise of wetland surface, ground water supply was cut off, and oligotrophic plants dominated. Their decomposition lead to bog formation.

The dominant type of bog in Meenikunno is *Sphagnum fuscum* that comprises 37 %, next one is *Eriophorum* – 13.8 %. The ash content of Meenikunno bog varies between 0.5 - 15.5 % (Salo et al., 1985).

The bedrock in the Meenikunno area consists of sandstone of the Devonian Gauja Regional Stage, which is overlain by 15 - 20 m of Quaternary glaciofluvial and glaciolacustrine sediments (Kink et al., 1996). The bog is surrounded by kames with relative height of 5 m. These spread SW and SE from the bog.

2.3. Ilumetsa impact research

Close (~6 km W-SW) to Meenikunno bog, the Ilumetsa site with at least two crater-like features (Põrguhaud and Sügavhaud) are located (Figs. 1 and 2).

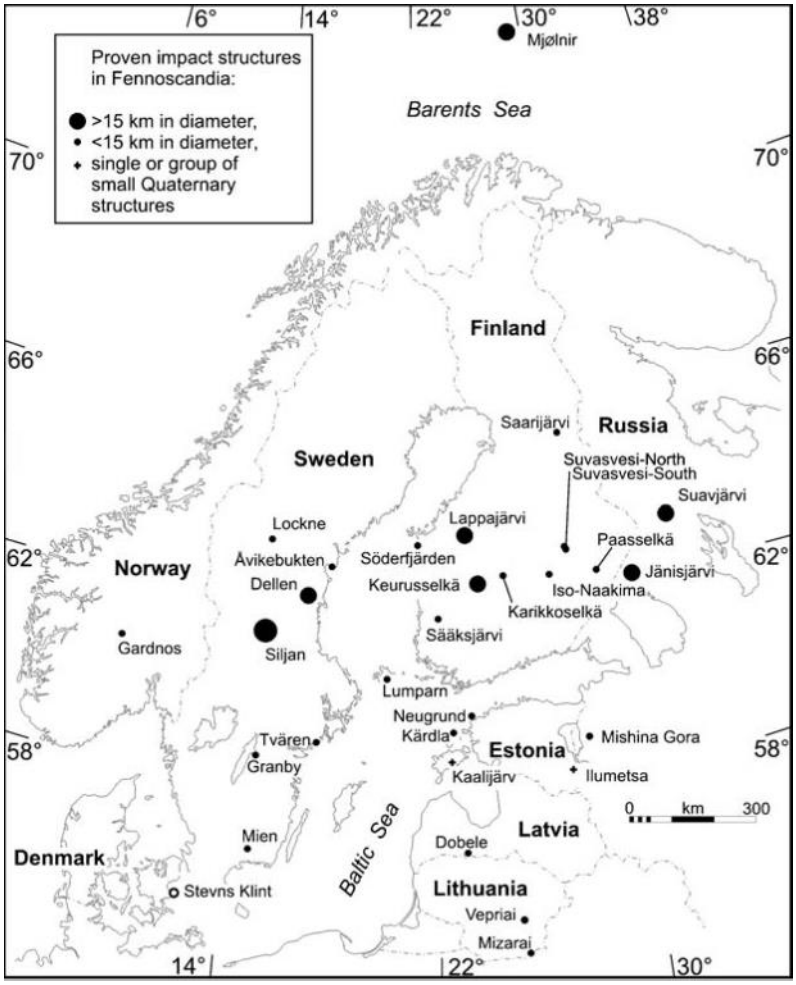

Figure 2. Recognized impact structures in Scandinavia and the Baltic states (Dypvik et al., 2008).

Artur Luha was the first to notice and study crater-like structures during the geological mapping course in 1938. Based on the structure of the Põrguhaud hole, he reached a conclusion that it might be a meteorite crater. To understand the morphology of Põrguhaud and find the evidence to support its meteoritic origin, Evald Pobul carried out magnetometrical measurements in Põrguhaud (1952), however; no magnetic anomalies were revealed. Ago Aaloe continued with research in 1956. In spite of that meteoritic iron was not found, he still concluded that Ilumetsa craters formed from iron meteorite, and that the material left was fully oxidized (Aaloe, 1960).

Põrguhaud, the largest crater, has a diameter of 75 – 80 m at the top of the uplifted rim, and is 12.5 m deep. The crater is partly filled with a thin layer of gyttja and peat that is up to 2 m thick. Radiocarbon ages of 6030 ±100 (TA-310; 6600 - 7250 cal BP) and 5910 ±100 (TA-752; 6450 - 7000 cal BP) year BP from the lowermost organic layer and palynological

evidence suggest that the structure formed some 7000 ^{14}C year BP. Not far (~700 m) south of Põrguhaud another crater is present; it is ~50 m in diameter and ~4.5 m deep Sügavhaud. Its bottom is covered by ~2 m thick sandy diluvium (Raukas et al., 2001; Stankowsky et al., 2007).

Raukas et al. (2001) investigated glassy spherules in nearby Meenikunno bog. During this investigation, twelve hand-drilled cores were obtained, with a Belarus peat corer, at intervals of 5 cm. Samples collected from these cores were divided and used for palynological, radiocarbon, and spherule analyses. For spherule analyses, the samples were ashed at a temperature of 700 ±25 °C. The ash was removed and the spherules were collected under a binocular microscope. Spherules were studied by means of a scanning electron microscope and microprobe analyses. Spherules were found only in one layer at the depth of 5.70 m.

Despite the thorough research, these spherules cannot be used as a trustful marker of their meteoritic origin. The research paper does not contain a description of the appearance and quantity of the findings, as well as it lacks correspondent photos and decent chemical analysis. Everything concluded, there is a need for a new research of mineral component preserved in Meenikunno peatland.

2.4. Microtektites

Tektites are natural glasses that have been formed in an impact event by the ejection of melted and/or vaporized near-surface rocks. The common size of tektites is of the order of centimetres defining the special group of microtektites that are less than 1 mm in size. Microtektites are mostly spherical in shape, but splash forms like ellipsoids, dumbbells, teardrops, and discs are also common. Sometimes the non-spherical shapes are considered to have developed due to the breakup and spin of melt droplets as they get transformed from melt to glass (Simonson, 2003).

In contrast to the mostly black, green, brown, or grey tektites, microtektites are transparent yellowish to brownish and even colourless. They may have very strange surface features and bizarre forms exhibiting micrometer-sized glass filaments and twisted bodies (Ernston, 2014).

Internally, unaltered impact spherules consist of glass with or without crystalline phases. The important distinction between these two types of spherules was first codified by Glass and Burns (1988) who coined the term microkrystite for spherules containing primary crystallites

and restricted the term microtektite to impact spherules that consist entirely of glass. Although this worked well for younger spherule layers that were not extensively altered, it is more difficult to apply to older layers in which crystals and/or glass can be replaced by secondary phases.

Microtektites and microkrystites are derived largely from target materials, i.e., terrestrial sediments and/or rocks. However, microkrystite generally have a higher content of extraterrestrial material than microtektites, judging from the fact that they are commonly associated with higher levels of iridium and other PGEs (Glass et al., 1999). The glass found in impact spherules such as microtektites differs from volcanic glass in a number of ways. Most notably, it has very low water content and iron is mostly in the Fe^{2+} state (Glass, 1990).

3. Methods

3.1. Ground penetrating radar

Ground penetrating radar (GRP) technique is based on high-resolution near-surface sounding of the ground. It is useful to map and outline Quaternary deposits like peat. In order to achieve that, the radar generates a pulse of electromagnetic (EM) energy that is transmitted into the ground. The subsequent propagation of the EM signal depends on the electrical properties of the ground. Any changes in these properties lead to the partial reflection of the transmitted signal. The reflections are recorded and amplified by the receiving antenna. The GPR system consists of the transmitter, receiver, control/display unit, and accumulator. Altogether, these measure the travel time of the EM signal. The measurements can be conducted at various frequencies depending on range and resolution required (Conyers, 2006).

The velocity of EM signal travel in the ground can be defined by individual constant for each material. It is called relative dielectric permittivity (RDP). The higher the RDP, the slower EM waves travel through. Difference between the values of the RDP of various geological materials is the key concept of GPR technique. For example, the RDP of water equals 80, while dry materials have only 4 - 8 (Davis & Annan, 1989). Relative dielectric permittivity of peat is 50 - 70, depending on peat type (Theimer, 1994). It explains the dependence of EM wave velocity on the water saturation in the ground.

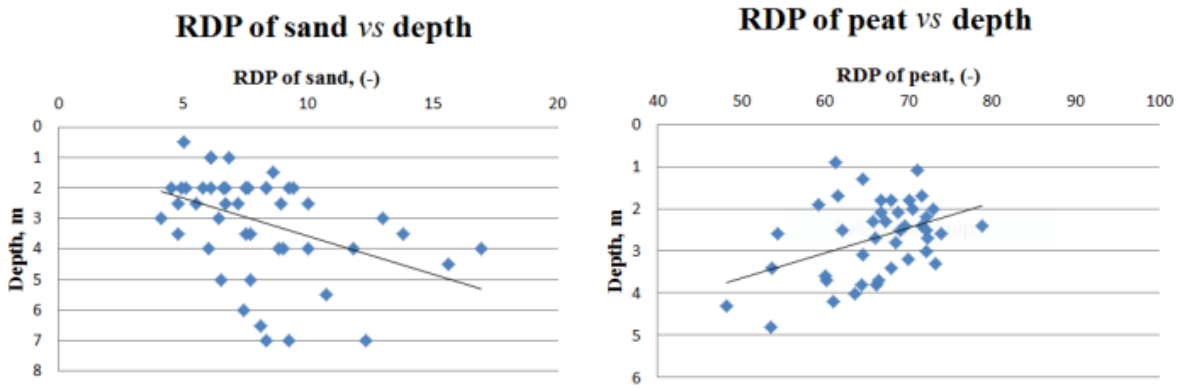

Figure 3. Relative dielectric permittivity (RDP) compared to the depth of peat and mineral deposits as based on the electromagnetic signal reflections from hyperbolic features in radar images.

The field measurements were conducted in August and October 2014. The GPR field work of Meenikunno bog was performed with a Zond 12-e system by Radar Systems Inc. The GPR signals were triggered by an odometer wheel and automatically coordinated with GPS. The data was received from 300 MHz frequency pulses. The time window for peat was 500 ns, whereas for sandy forest areas 200 ns.

The data were processed with the Prism2 software (Radar Systems, Inc., 2005). Ormsby band-pass filter, gain function, and time-depth conversion were used for a better visualization. The EM signal reflections from hyperbolas were used to calculate the mean permittivity and velocity for both: peat and mineral deposits. The mean permittivity for peat is 66.2, and EM wave velocity is 0.037 m /ns, whereas for mineral deposit it is 8.0 and 0.106 m /ns, respectively (Fig. 3). The peat and mineral soil boundary was defined by strong EM signal reflections and marked manually every 10 m. An initial map of peat thickness was compiled to locate future drilling positions.

In the second part of the field work conducted in the mid of October 2014, a peat-drilling was performed. Three main drill cores (MEEN-P1, P2, and P3) were described at their total length. Lowermost sequences were sampled as one-meter long cores for further analysis (see Chapter 4.1). MEEN-P4-1 and P4-2 were drilled in attempt to access deeper peat layers. The distance between P4-1 and P4-2 was approximately 1 m.

After the field work in Meenikunno, an interpolated map with peat depth distribution was compiled. The coordinates (L-EST97) of peat coring location in MEEN-P1 are 697017E;

6427398N; MEEN-P2 - 696992E; 6427154N; MEEN-P3 - 696601E; 6426939N; and MEEN–P4 - 697037E; 6427407N (see Chapter 4.1).

3.2. Magnetic susceptibility

Magnetic susceptibility (χ) is a value that reflects the degree of magnetization of the specific material in response to an applied magnetic field. In SI, χ is the dimensionless unit and exists in either positive or negative value. If χ is negative, then it is the sign of diamagnetic material; positive χ is due to para- or ferromagnetic materials. To identify possible mineral layers, magnetic susceptibility of sampled peat was measured with portable MS3 Magnetic Susceptibility Meter at every 1 cm along the cores. The received data were automatically recorded with the help of Bartsoft software. The results were plotted as a proxy with χ versus depth (see Chapter 4.2).

3.3. Inorganic material removal from peat samples

To separate non-organic particles from peat, two methods, (i) physical organic component removal by burning peat samples and (ii) chemical organic component removal by using hydrogen peroxide (H_2O_2), were used.

First, peat core sections were cut with plastic knife along the longer axis for two equal parts. One of the parts was divided for 10 cm long sections. Then, samples were weighted (m_w) and put for an excess moisture removal at 105 °C for 24 h. After that, there was a new weighting procedure (m_d) and then heating again, although this time at 550 °C and for 4 h plus 1 hour to get the right temperature in the oven. According to the weighting results, the loss on ignition (LOI) was calculated (Santisteban, 2004):

(1) $LOI_{105} = 100\frac{(WS - DW_{105})}{WS}$,

where WS is the weight of the air-dried sample and DW_{105} is the dry weight of the sample heated at 105 °C and

(2) $LOI_{550} = 100\frac{(DW_{105} - DW_{550})}{WS}$,

where LOI_{550} is the percentage of loss on ignition at 550 °C and DW_{550} is the weight of the sample after heating at 550 °C.

The ash that remained after the burning of the peat samples was collected into flasks with distilled water. Then, it was stirred to ensure the preliminary separation of light (ash) and

heavy (mineral grains) particles. The lighter were removed, whenever possible. The “residue” was poured into conical paper filters, and left until most of the water was eliminated. These filters were later examined by the binocular microscope, and the mineral grains were collected by hand. The findings had to undergo cleaning with water and ultrasound in order to be photographed.

Another half of long sections was selectively (based on findings resulting from peat burning experiment) cut into 1 cm long sections. These samples were placed into individual flasks with hydrogen peroxide (H_2O_2) and heated in the temperature range of $70 - 90\,^{\circ}C$ to accelerate chemical decomposition of peat. Next, the processed samples were separated from the H_2O_2 with help of conical paper filters, washed, and viewed under the binocular microscope. As a result, the findings from this procedure were collected and photographed.

3.4. Optical mineralogy

For a quick overview of the mineralogical properties of the mineral findings, an oil-immersion method was used. The grains from the samples were covered with a drop of immersion oil and distributed over a transparent glassy plate that was able to transmit the light. The grains were observed both at plane- and cross-polarized light. The latter was more informative as it helped to distinguish whether the grain has a crystalline or amorphous structure. While mineral grains with crystalline lattice often show high-interference colours under the cross-polarized dim, the amorphous ones, such as glasses, express constant extinction.

3.5. Geochemistry

3.5.1. SEM-EDS

Scanning electron microscopy (SEM) along with energy dispersive X-ray spectroscopy (SEM-EDS) is a non-destructive tool for surface analysis. A scanning electron beam glides across a sample's surface, and when its electrons strike the surface, specific signals are generated and detected. These signals produce a high-resolution image of sample's topography and/or its elemental composition. Most of information is provided by secondary/backscattered electrons and X-rays.

With secondary electrons, image contrast is determined by sample morphology. The intensity of backscattered electrons can be correlated to the atomic number of the element within the

sampling volume. Hence, some qualitative elemental information can be obtained. Interaction of the primary beam with atoms in the sample causes shell transitions which result in the emission of an X-ray. The emitted X-ray has an energy characteristic of the parent element. The analysis of characteristic X-rays (EDS analysis) emitted from the sample gives more quantitative elemental information.

Non-conductive specimens tend to charge when scanned by the electron beam. Such specimens may however be imaged uncoated using environmental SEM (ESEM) or low-voltage mode of SEM operation (Hortolá, 2005). Low-voltage operation below 5 kV has improved X-ray spatial resolution by more than an order of magnitude and provided an effective route to minimizing sample charging (Goldstein, 2003).

The examination of the selected samples was carried in SEM laboratory (University of Tartu) with Zeiss EVO MA15 scanning microscope. It is equipped with various detector systems like Oxford Aztec X-MAX 80 EDS Röntgen fluorescence analyser that make it possible to obtain an electronic image with high level of magnification and high resolution (up to 200,000 ×).

The samples were left uncoated as they were studied in low vacuum regime. The elemental analysis of samples' surface was done with integrated EDS software that automatically proposed chemical elements for the "peaks" found. Nonetheless, a manual assistance helped to achieve more logical results.

3.5.1. ICP-MS

Trace element analysis of sample Meen_P3_5.5-5.6 were performed by LA-ICP-MS (laser ablation inductively coupled plasma mass spectrometry) using Cetac LSX-213 G2+ laser built around a two-volume HelEx sample cell connected to Agilent 8800 Triple Quadrupole ICP-MS. Stable isotopes of Si^{28}, Fe^{56}, Co^{59}, Ni^{60}, Ru^{101}, Rh^{103}, Pd^{105}, Os^{189}, Ir^{193}, Pt^{195} were measured from spot analysis and results were quantified using NIST 612 and NIST 610 reference materials, using Si as the internal standard and the SiO_2 concentration in the glass sphere was assumed to be 99%. He was used as the carrier gas for sample transport and the ablation parameters were as follows: laser spot size 40μm, pulse repetition rate 5Hz and fluence (energy density) $5J/cm^{-2}$. Data reduction was performed using Glitter Software.

4. Results

4.1. GPR and peat stratigraphy

A prominent reflector, that originates from the boundary between the overlying peat (and gyttja) and the underlying lake sediments (sand), was detected and delineated. In some cases the reflection disappeared at depths greater than 6 m, but still, the maximum thickness observed by GPR study was as high as 7.92 m. In the margins of the bog, thicknesses are generally the lowest, while in more central part, especially close to Keskmine- and Suur Suujärv lakes – the highest values are present. These high values are elongated along a NE-SW trending furrow in the middle of investigation area (Fig. 4). The five drillings, close-by to GPR profiles, did not contradict the depth interpretations, but showed occurrence of steep slopes of below-peat topography (Fig. 5a-c).

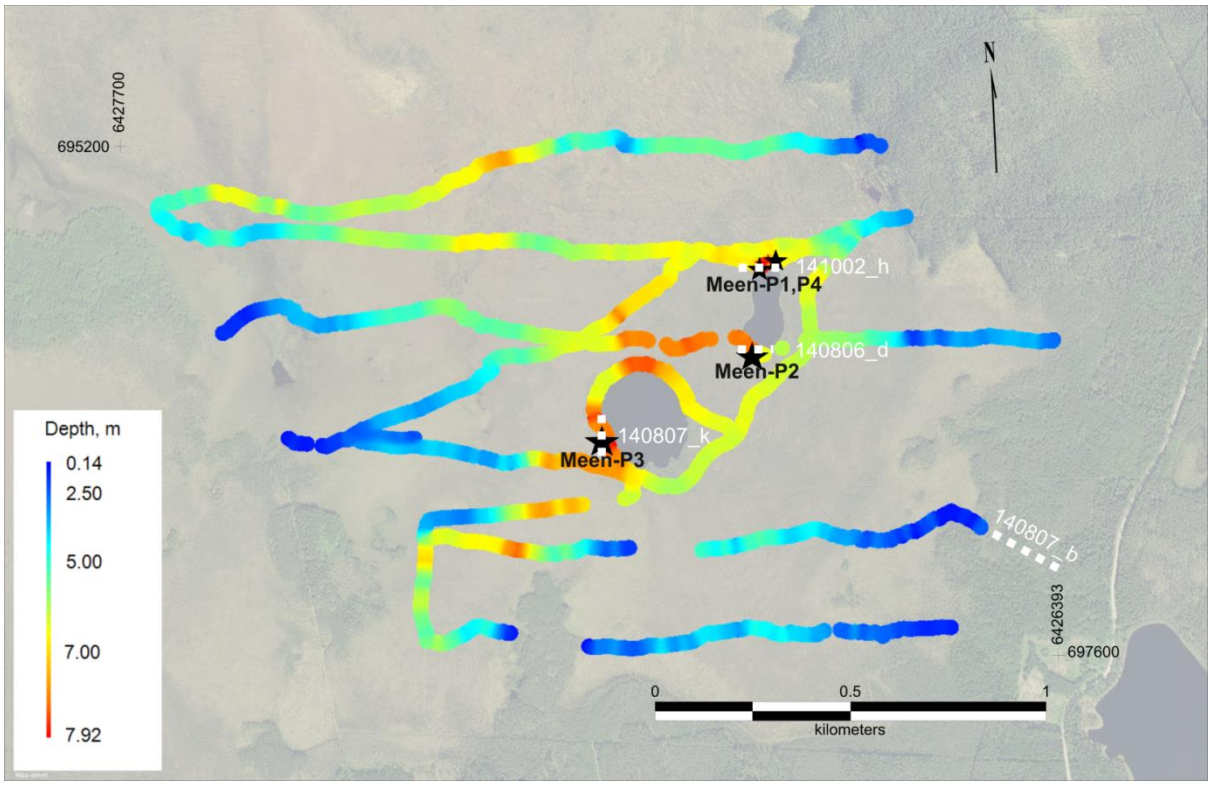

Figure 4. Map of peat depth in Meenikunno as based on ground-penetrating radar studies. Peat coring sites (MEEN-P1, P2, P3 and P4) are marked with black stars. Orthophoto for map`s background was obtained from Estonian Land Board (X-GIS).

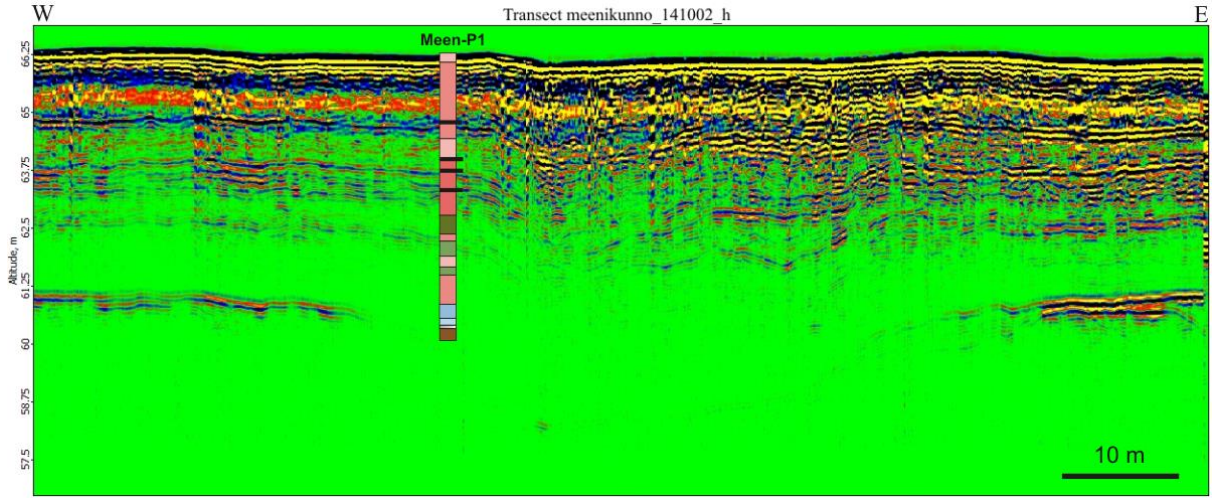

Figure 5a. Location of the drill core Meen-P1 on a radargram meenikunno_141002_h (696797E; 6427408N – 696900E; 6427413N). The vertical scale is exaggerated 4.4 times.

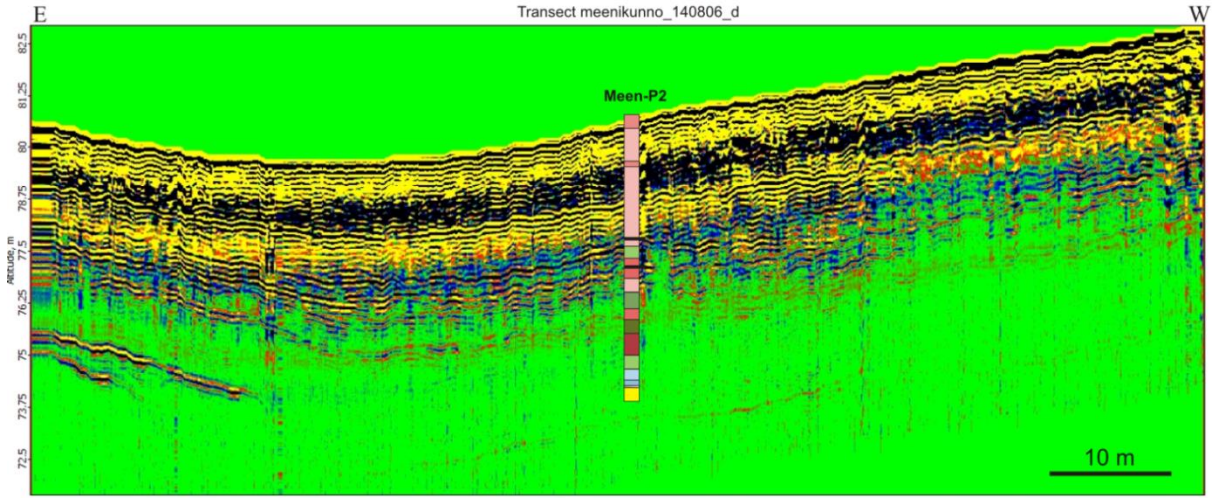

Figure 5b. Location of the drill core Meen-P2 on a radargram meenikunno_140806_d (696436E; 6427148N – 696698E; 6427207N). The vertical scale is exaggerated 3.2 times.

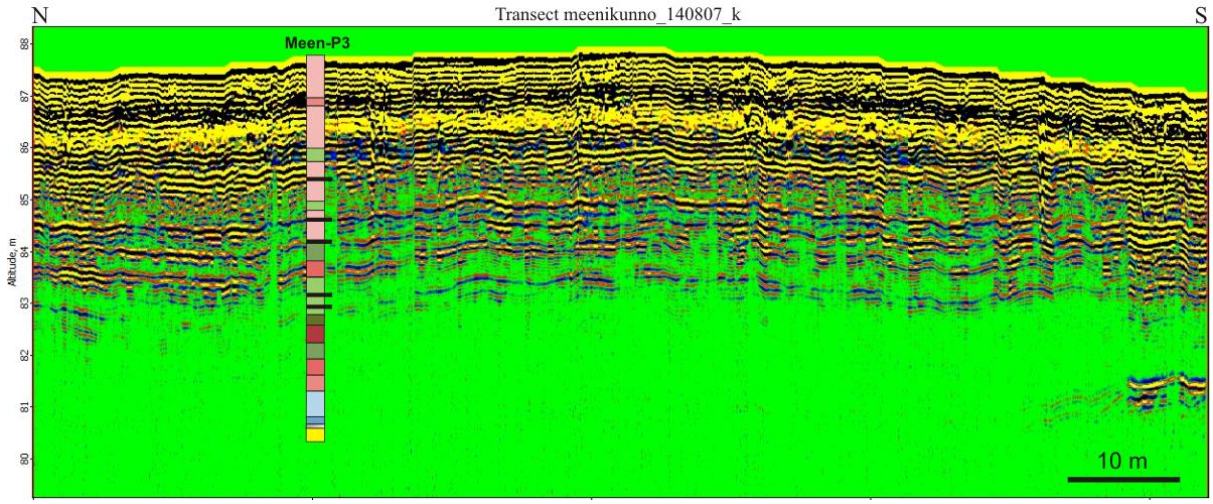

Figure 5c. Location of the drill core Meen-P3 on a radargram meenikunno_140807_k (696445E; 6426961N – 697402E; 6426727N). The vertical scale is exaggerated 4.4 times.

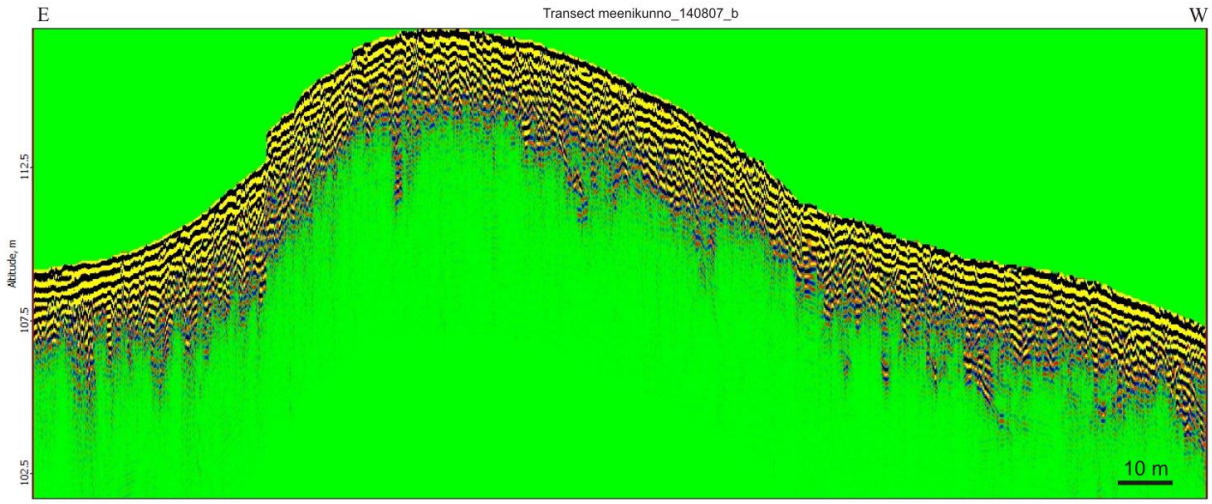

Figure 5d. Radargram meenikunno_140807_b represents the surrounding area of Meenikunno bog (696436E; 6426721N – 697402E; 6426727N). The vertical scale is exaggerated 12.5 times.

Generally, there is a good correlation in terms of peat types among all drilled cores. There are several marks of peatland fires in Meenikunno. One of the burned peat layers has almost the same depth: 2.33, 2.28, and 2.34 m for Meen-P1, 2, and 3, respectively. Another, yet slightly less matching is the layer at the depth of 2.96, 2.85, and 3.11 m. A reasonable good overlap of coal layers with sharp reflections in radar images occurs.

There are also EM wave reflections that do not match the depth of burned peat layers. For example, these are found at the altitude of 62.5 m for Meen-P1 and 76.25 m for Meen-P2. It could be due to i) during the *in situ* observation, the burned layer was not identified; ii) it shows the transition between bog and sedge mire; iii) it reflects the increase in decomposition rate of peat. If the last suggestion is true, then it means that peat layers with higher decomposition rate can be spotted more easily that those with lower rate, and they cause stronger EM wave reflections. No any signs of spherule layers or their concentration were spotted by GPR method.

The surrounding area of Meenikunno bog is illustrated on Fig. 5d. It shows relatively homogenous layers of clayey sand, which screen EM waves and reveal only little depth of the underlying deposit.

Peat types of Meenikunno were divided into three main groups (see Fig. 6 and Appendix 1): *Sphagnum-Eriophorum*, wooden and *Equisetum-Carex*. Exactly this order of peat types describes their distribution from the top to the bottom of peat cores. *Equisetum-Carex* group

is the lowermost, and can be linked to the poor fen stage of Meenikunno peatland development. All main drill cores and Meen-P4-2 have on average 53.3 cm long peat core sections in this group. *Sphagnum-Eriophorum* group dominates on top of the sections, and then alternates with wooden group. The transition between bog and sedge mire stage is not very evident except core Meen-P3, where it was marked at the depth of 6.3 m.

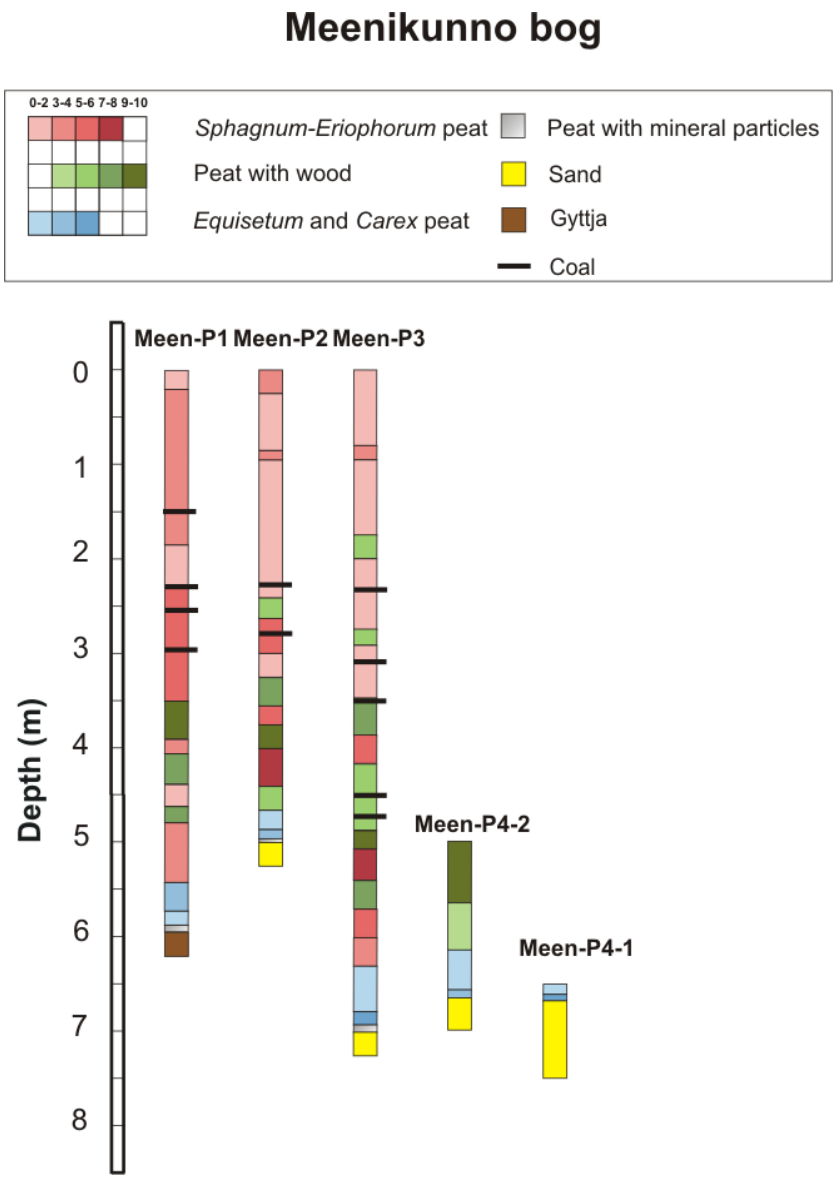

Figure 6. Stratigraphic columns and legend of Meenikunno peat core sections. It is a generalized illustration of information from Appendix 1.

4.2. Magnetic susceptibility and LOI of peat

The measurement of magnetic susceptibility (χ) was conducted to identify possible depth of microtektites with apparent magnetic properties. In fact, no such location was found as χ values of peat cores were quite low. They stayed in a range of -30 up to -5 SI, thus reflecting paramagnetic properties of peat. Some small peaks in the direction of higher χ values were noticed: Meen-P1 (3.5; 5.3 m), P2 (4.0; 4.7 m), and P3 (3.0; 3.45; 4.0; 4.8 m); however, no evident correlation between this and number of findings or the presence of burned layers was found (Figure 7). A general increase of χ with depth in lower parts of sections can be attributed to increasing content non-organic material.

On the basis of the weighting results, three graphs concerning LOI were built. Figures 8a-c shows that: i) moisture content of peat decreases with depth; ii) organic component rises with depth; iii) the percentage of ash content and mineral particles of peat increases with depth.

The graph on Figure 8a is a mirror image of Figure 8b, as the more weight of peat is comprised of water content, the less is left for organics. The organic content is higher

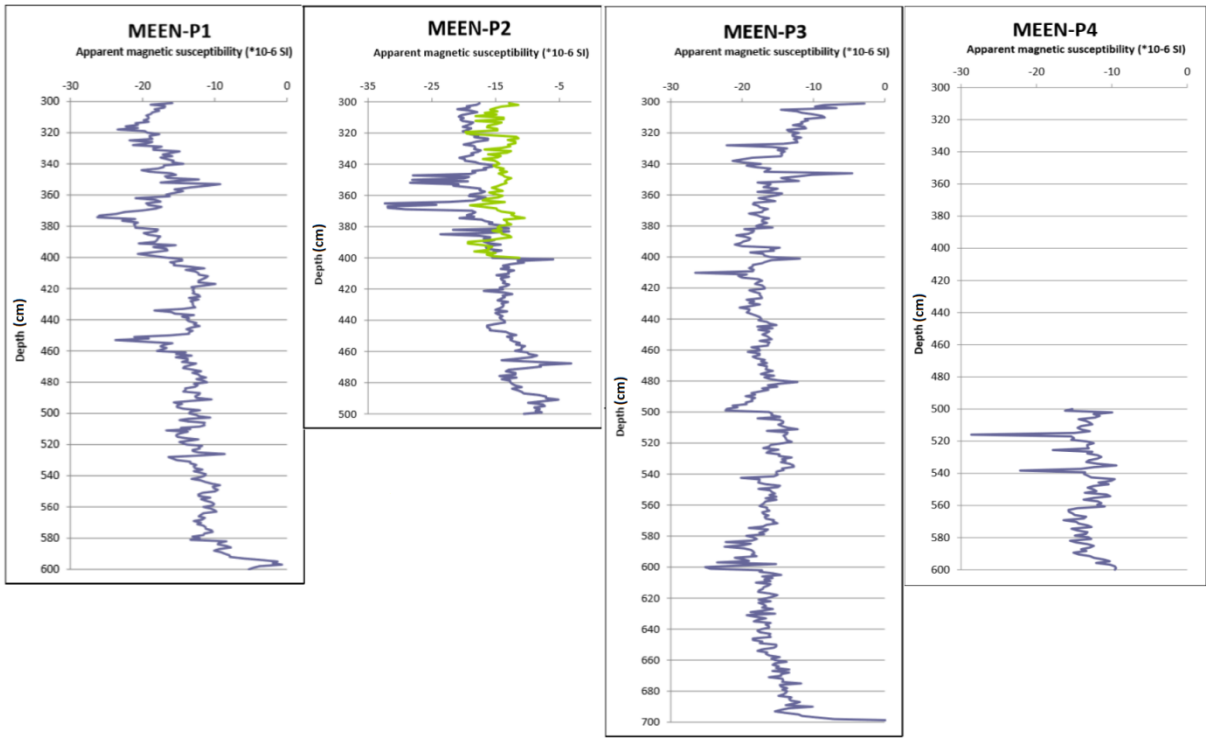

Figure 7. Apparent magnetic susceptibility of Meen-P1, P2, P3 and P4 peat core sections. The upper segment of Meen-P2 (300-400 cm) was done twice due to the doubtful initial values.

downwards, as peat layers tend to thicken with depth. The ash content is higher in lower peat sections than in the upper, because the lowest layers are more reliant on the topography of the underlying base (sediments). Water flows can transport mineral particles towards depressions, and concentrate them in the lowermost layers.

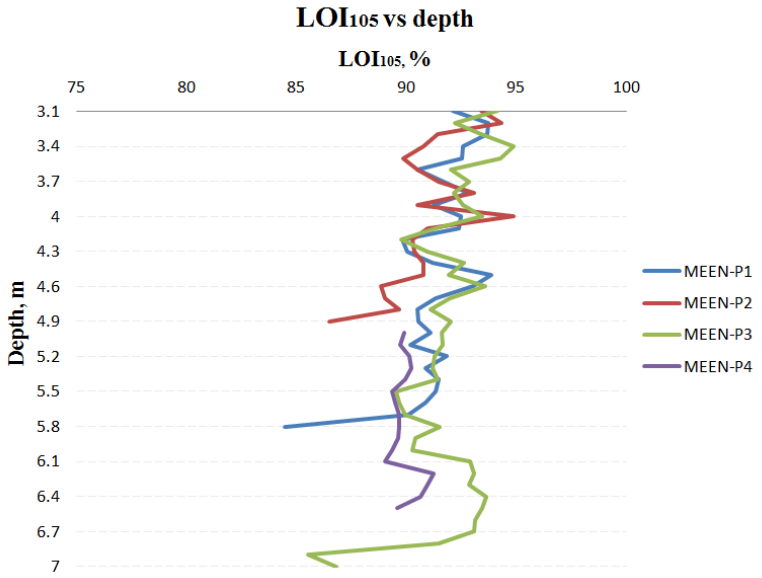

Figure 8a. Loss on ignition calculation after moisture removal from peat samples at 105 °C. For a better visualization of results the following sections were excluded from the graph: Meen-P1 (5.8-6.0 m), Meen-P2 (4.9-5.0 m), and Meen-P4 (6.6-7.0).

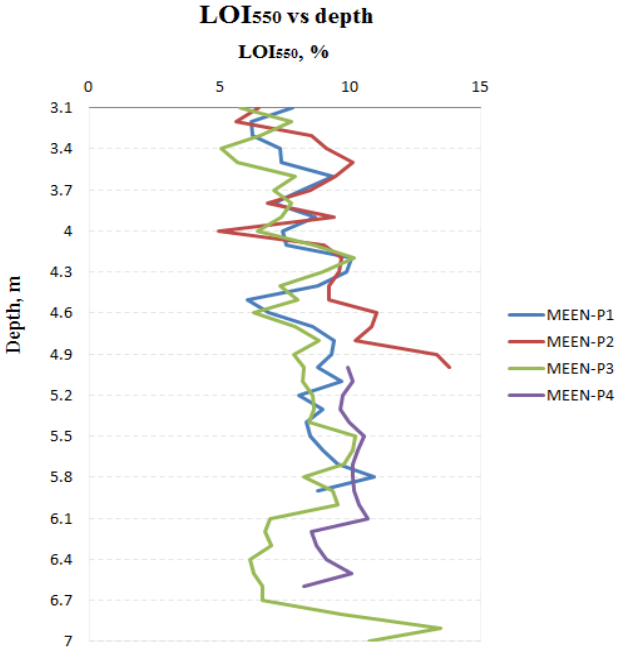

Figure 8b. Loss on ignition calculation after organics removal from peat samples at 550 °C. For a better visualization of results the following sections were excluded from the graph: Meen-P1 (5.9-6.0 m), Meen-P4 (6.7-7.0).

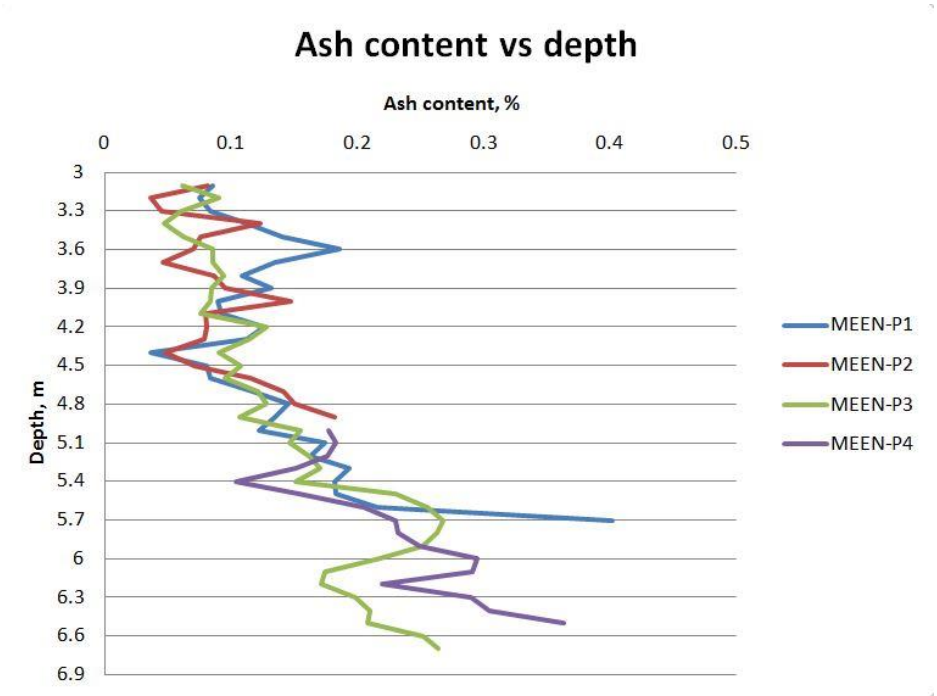

Figure 8c. The percentage of ash content and mineral particles of peat. For a better visualization of results the following sections were excluded from the graph: Meen-P1 (5.7-6.0 m), Meen-P2 (4.9-5.0 m), Meen-P3 (6.7-7.0), Meen-P4 (6.6-7.0).

4.3. Non-organic particles

Non-organic material from the Meen-P1 was found at five sections, with 4 of them in the lowermost part of the peat core. The ten findings were mostly transparent and angular. Meen-P2 was the shortest peat core, and it had five locations and only six findings that were very different from each other in terms of size, shape, and colour, but they were distributed evenly along the core. In Meen-P3, the longest of main peat cores, there were seven locations and 14 samples found. Most of the samples were transparent and angular. Meen-P4 was the smallest to describe (only ~ 1.5 m), yet it had much more grains than Meen-P1, 2, and 3 altogether. It had 14 locations with mostly transparent grains of different shape.

The majority of the findings were counted as sand grains. They definitely have various origin inferring from their properties. For example, grains with matte surface had likely aeolian type of transportation (Kalle Kirsimäe, pers. comm.). However, a thorough investigation on the origin of grains is conducted only for two of all the findings (see further chapters).

All in all, Figures 9a-d illustrate the findings, and correlate well with the results of magnetic susceptibility measurement and LOI, showing that number of findings, ash content, and χ trends increase with the depth along the peat cores.

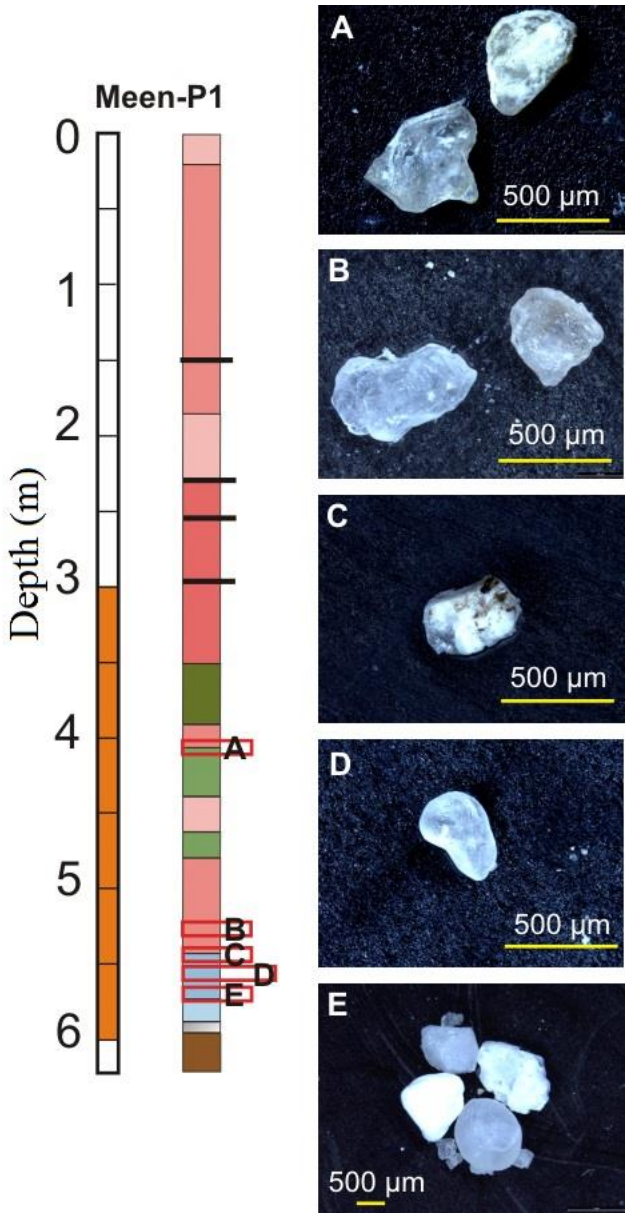

Figure 9a. The peat core section Meen-P1 and its non-organic material (A-E).

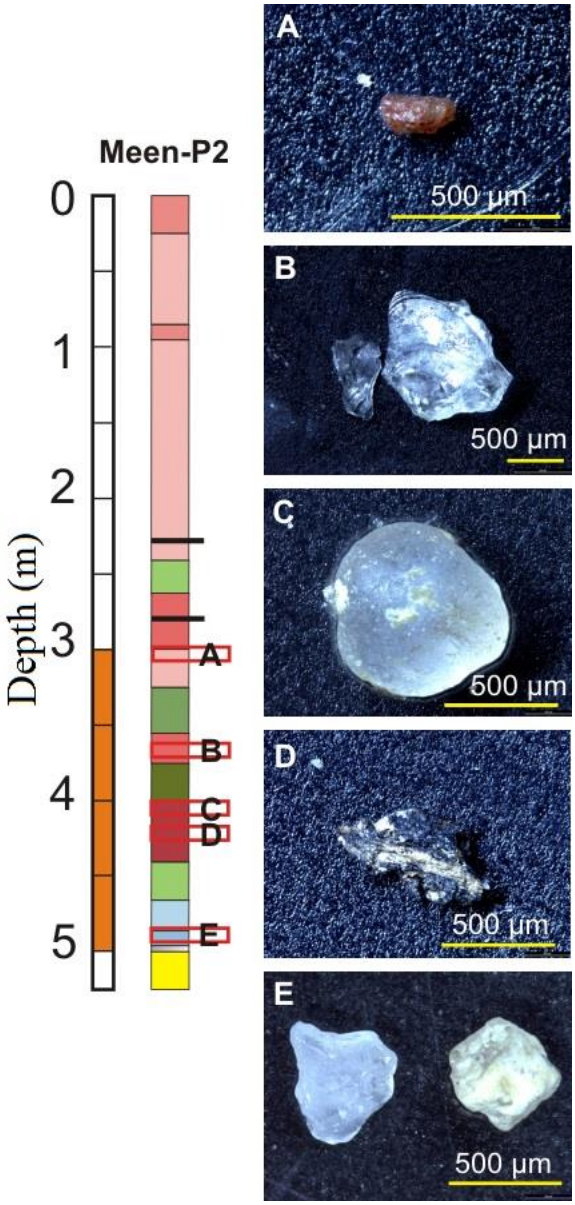

Figure 9b. The peat core section Meen-2 and its non-organic material (A-E).

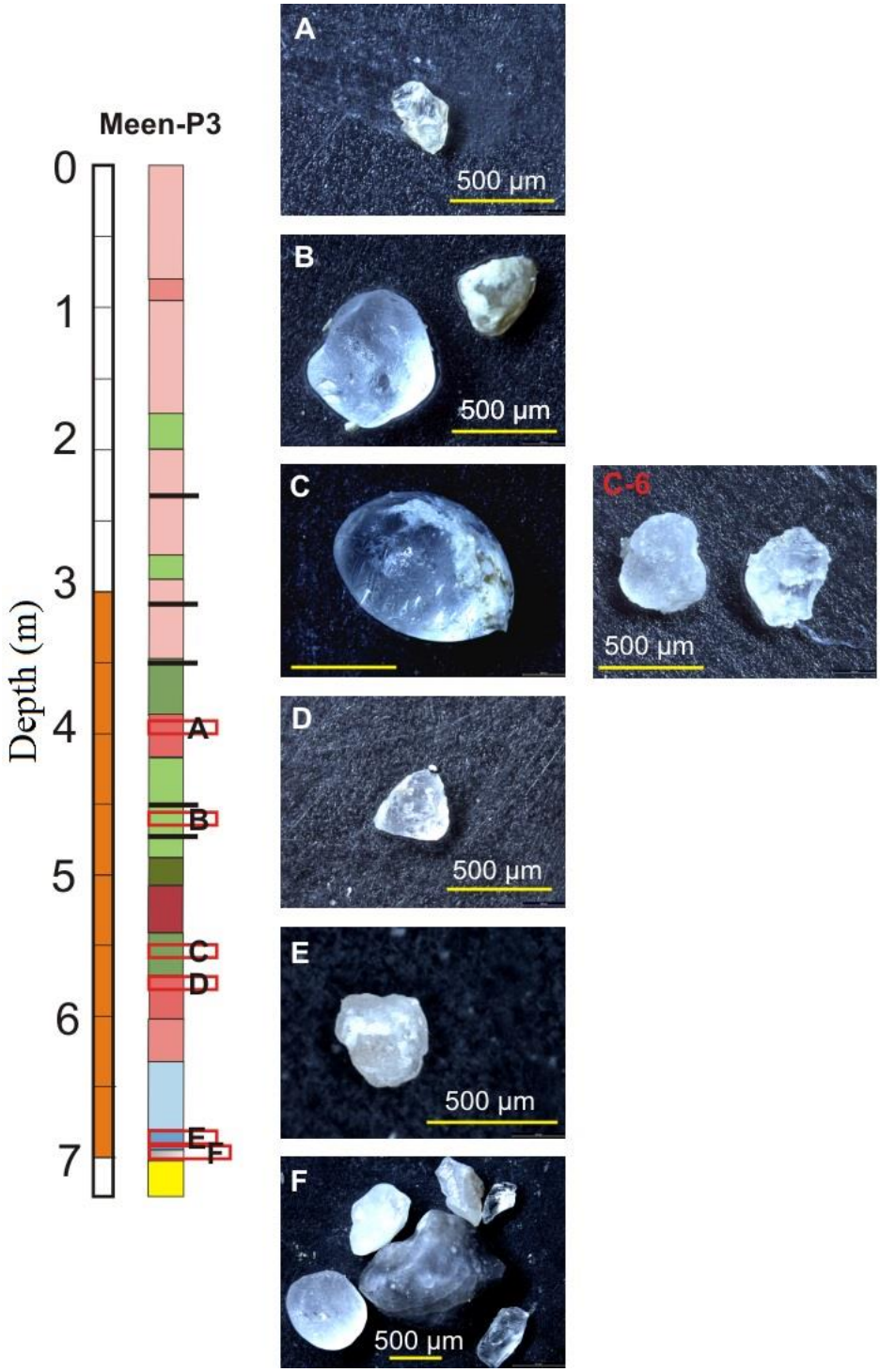

Figure 9c. The peat core section Meen-P3 and its non-organic material by burning (A-F) and by H_2O_2 method (C-6).

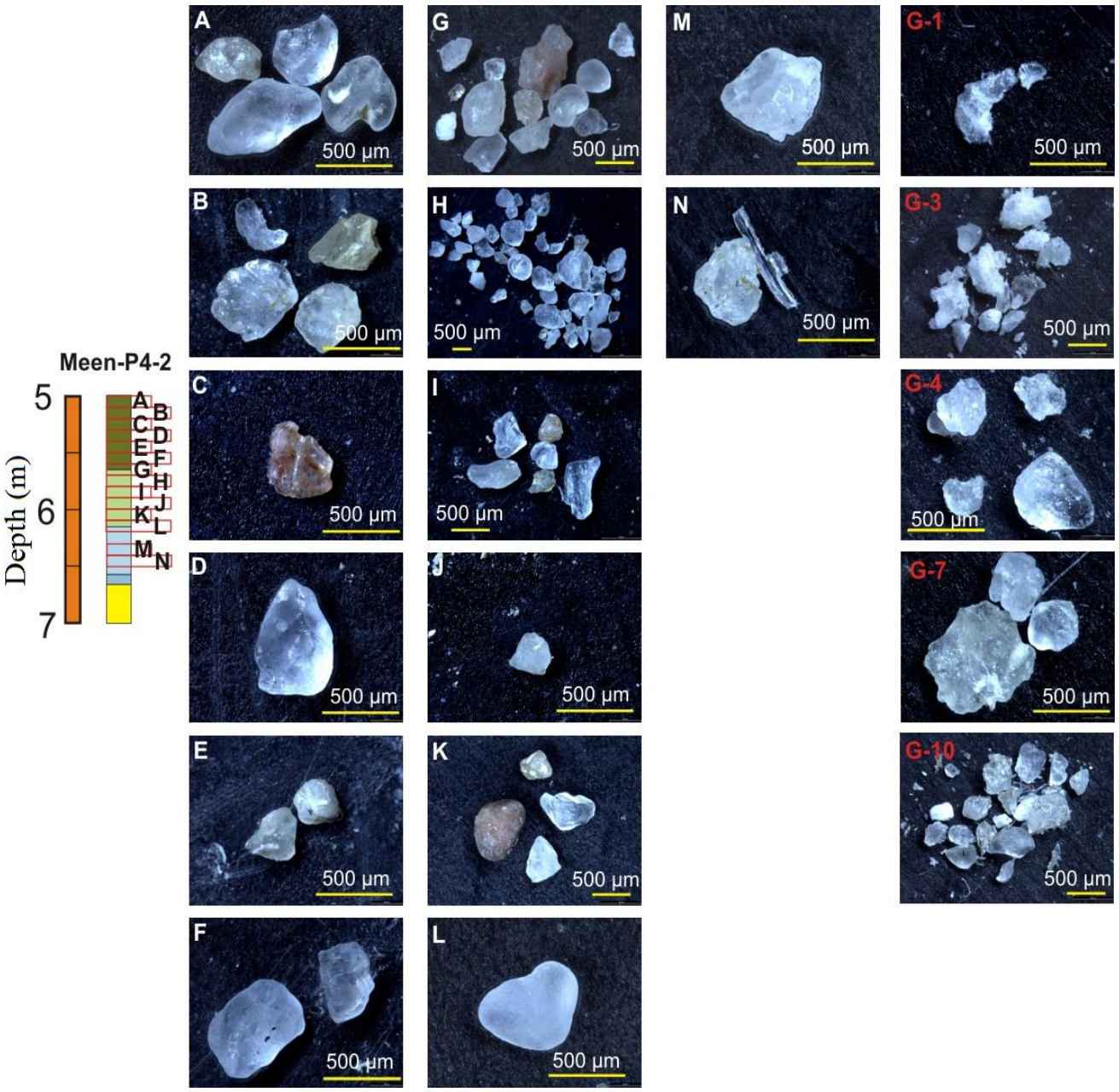

Figure 9d. The peat core section Meen-P4-2 and its non-organic material by burning (A-N) or by H_2O_2 method (G-1, 3, 4, 7 and 10).

4.3.2. Optical properties

To help the selection of findings for further geochemical analysis, the mineral grains were studied under an optical microscope with the oil immersion method. Two of the findings showed clear distinction under the cross-polarized light revealing their glassy, amorphous structure. The first one comes from the Meen_P2_3.6-3.7 and resembles a shard of transparent glass. The second one of Meen_P3_5.5-5.6 has different appearance: elongated and transparent sphere with inner bubbles (Fig. 10 A1-2).

The majority of the findings, like on Fig. 10C, showed their interference in cross-polarized light, so that they have crystalline structure. Some of the grains observed were probably too big, and thus thick for a good estimation of their optical properties, showing no interference and appearing as isotropic.

4.3.3. Chemical properties

Taking into the account shape, colour, surface features and optical properties, six findings from five depths (Meen_P4_5.2-5.3, P4_5.6-5.7, P4_6.0-6.1, P2_3.6-3.7, and P3_5.5-5.6 m) were selected for SEM-EDS analysis. During the analysis in low vacuum regime, the uncoated samples were charged with carbon. This sort of contamination makes the results

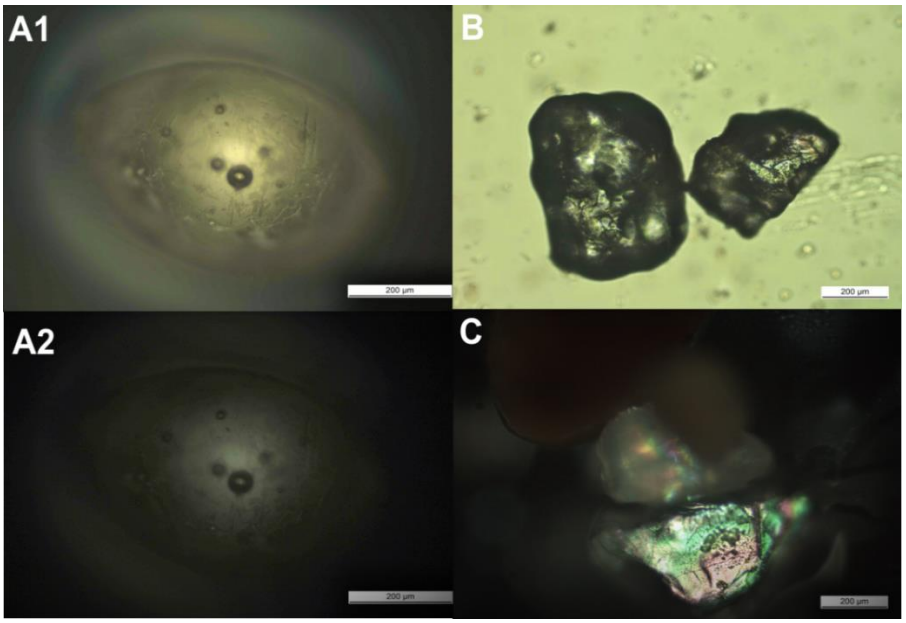

Figure 10. Example of mineral grains investigation under the optical microscope. (A1) Sample P3_5.5-5.6 in plane-polarized light. (A2) Sample P3_5.5-5.6 in cross-polarized light. (B) Sample P4_5.5-5.6 in plane-polarized light. (C) Sample P4_6.0-6.1 in cross-polarized light.

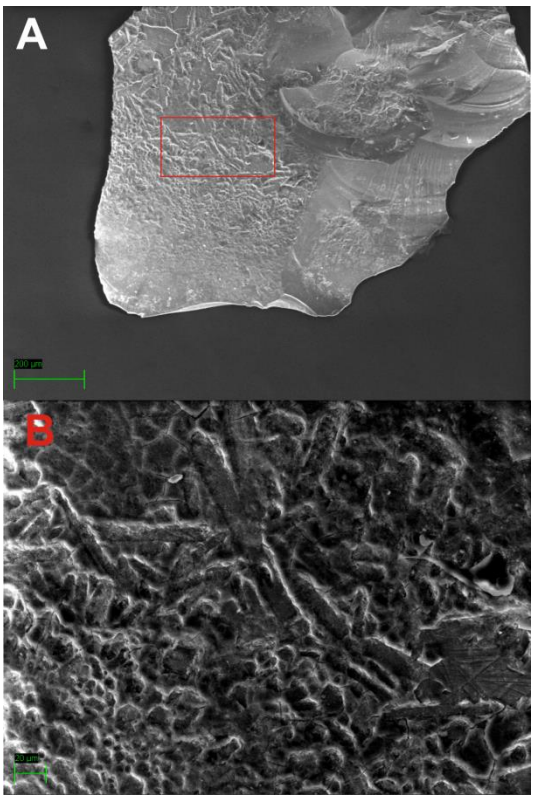

Figure 11. The SEM image of the sample from Meen_P2_3.6-3.7 m.

from the first attempt only be considered as indicative. In the repeated SEM-EDS analysis the samples were still charging, though to a lesser extent. It was decided to eliminate carbon as an element from the calculation of chemical composition.

After the first measurement and its results, the findings from Meen_P4_5.2-5.3, P4_5.6-5.7 and P4_6.0-6.1 m were classified as sandy grains. They contained high wt% of Si, O, and to some extent the elements like K, Al, and Na. In addition, SEM images indicated more detailed surface features of grains. Their surfaces were pitted, revealing that these grains were weathered before the final deposition in Meenikunno bog (Appendix 2a-d).

The most curious surface`s morphology is on sample Meen_P2_3.6-3.7. The sample itself is flat, angular and has two parts: left and right. The part on the left side has pitted surface that at closer look resembles some channels, whereas the right part consists of fracture zone (Fig. 11). This part with its rounded, conchoidal fracture reminds of obsidian.

The spectral analysis of Meen_P2_3.6-3.7 shows that it mostly consists of SiO_2; however, there is a number of other chemical elements like Ca, Na, K, Al, Fe, Mg, P, S, and P. It is

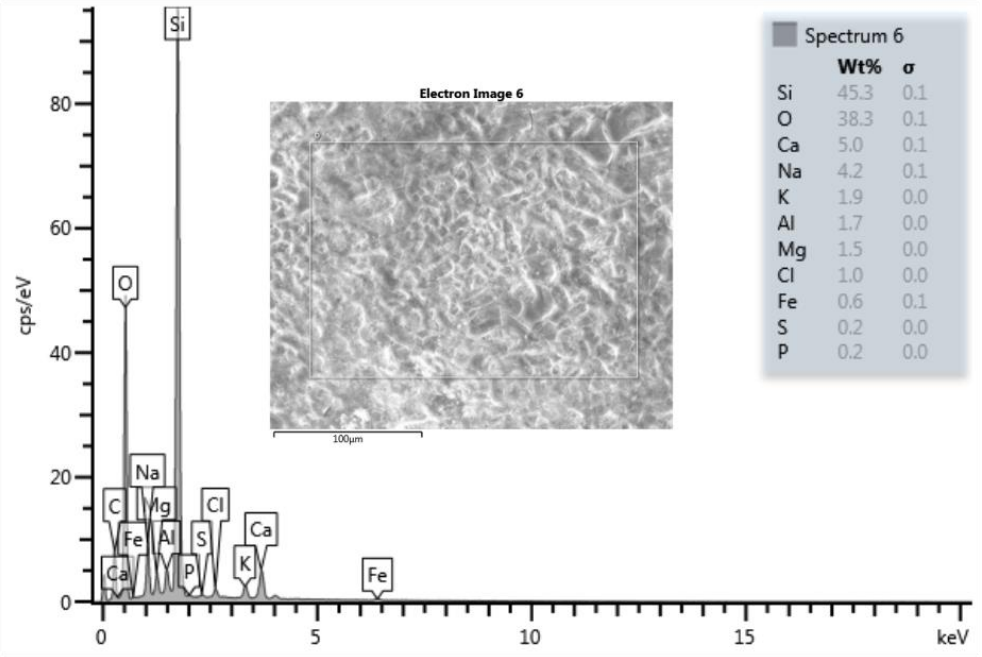

Figure 12a. Spectral analysis of the left part of Meen_P2_3.6-3.7.

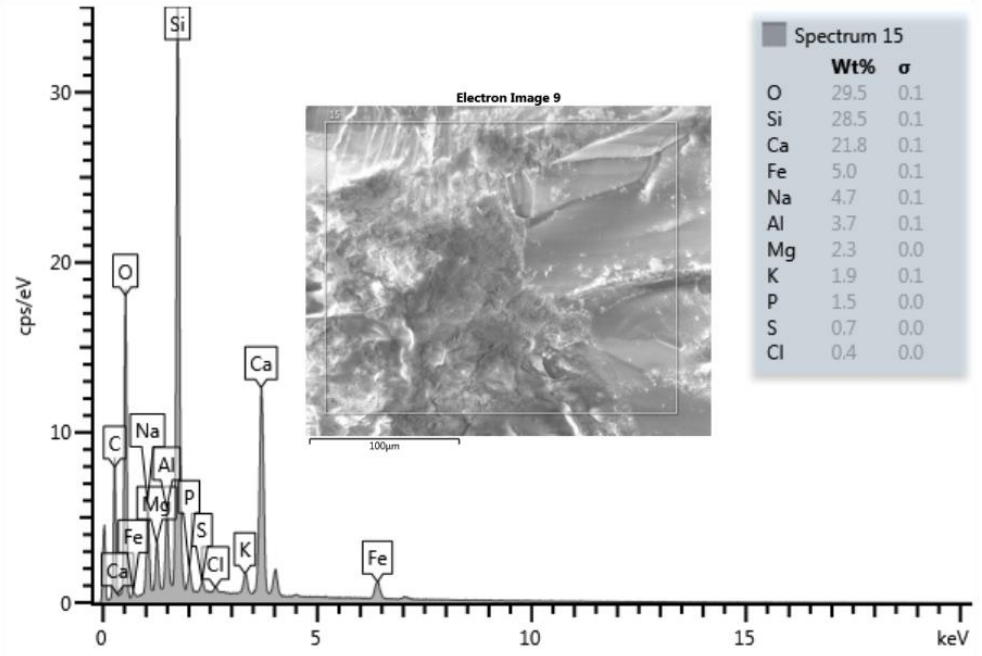

Figure 12b. Spectral analysis of the right part of Meen_P2_3.6-3.7.

interesting to trace their abundance in both: the left and the right side of the sample. The left spectrum is more enriched in Si and O, while the right one shows higher concentration in other elements, especially Ca, Fe, and P (Fig. 12 a and b). Probably, the right spectrum has more "fresh" surface that provides with more detailed precise chemistry.

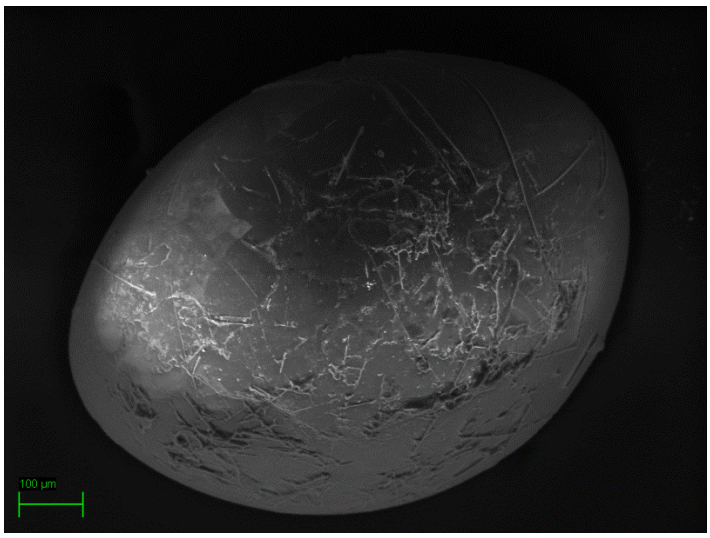

Figure 13. The SEM image of the sample from Meen_P3_5.5-5.6 m.

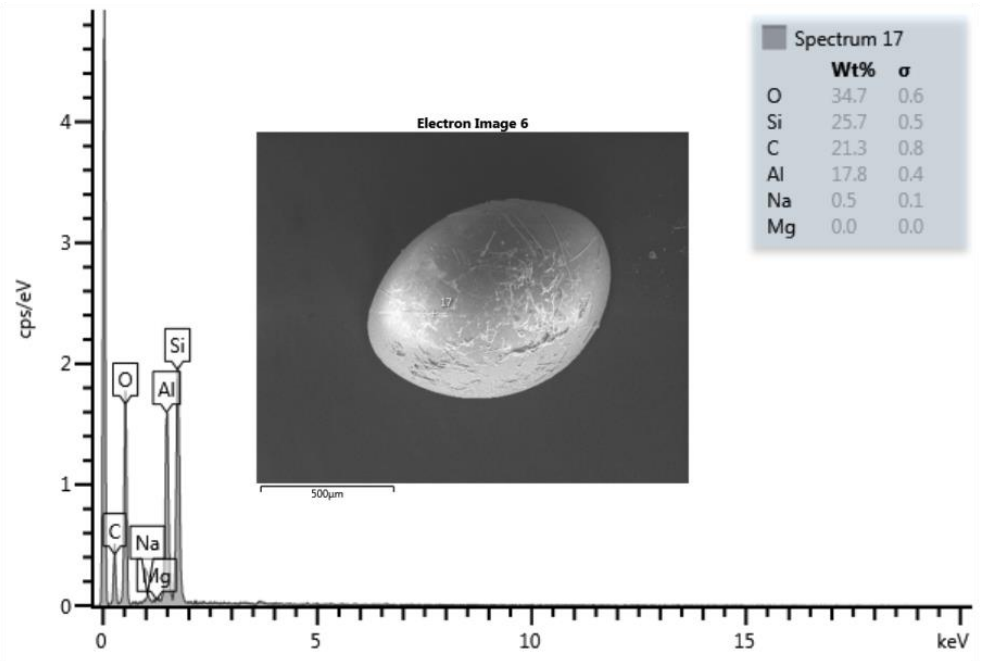

Figure 14. Spectral analysis of the sample from Meen_P3_5.5-5.6 m.

Sample Meen_P3_5.5-5.6 is the only one from all findings that has such an elongated, spheroidal shape (Fig. 13). Unlike ordinary picture where the air bubble are seen, SEM image gives a better look on surface`s morphology. The grains has generally smooth surface, but it is chaotically covered with very thin lines that sometimes intersect each other.

Although the spectral analysis of Meen-P3-5.5-5.6 is contaminated with C, it still shows the major elements present – Si, O, Al, Na (Fig. 14). ICP-MS trace element analysis detected the concentrations of Fe^{56}, Co^{59}, and Ni^{60} as 363, 0.8, and 5.8 ppm. Noteworthy is that

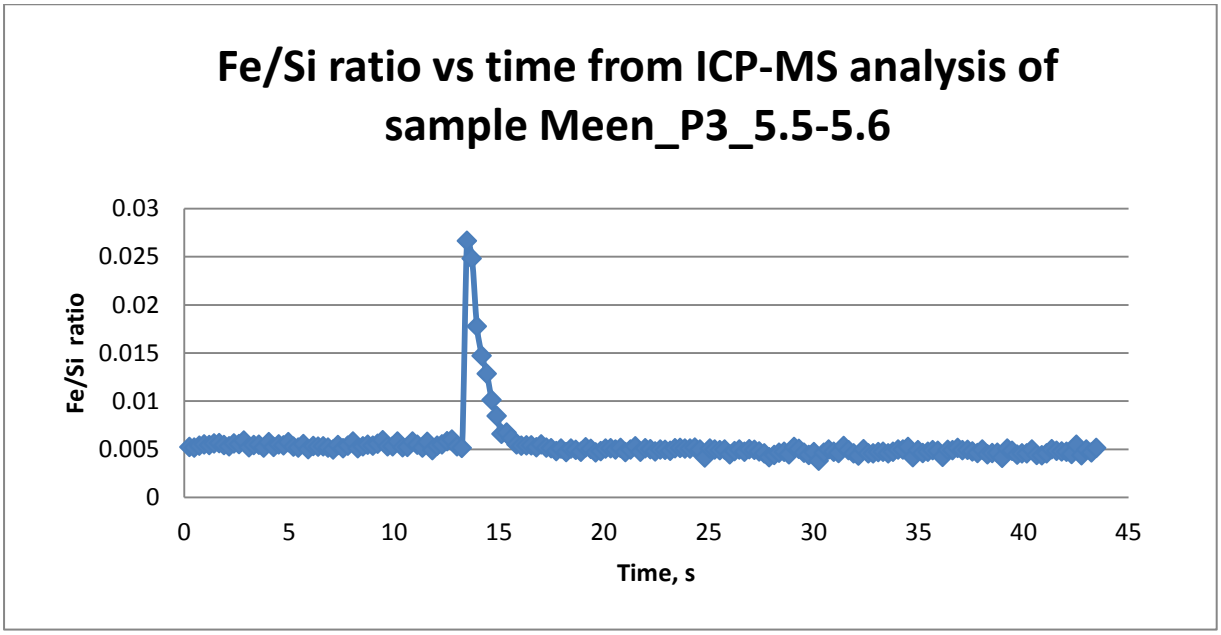

Figure 15. The Fe/Si ratio versus time during the ICP-MS analysis of Meen_P3_5.5-5.6 (By P. Paiste).

the Fe/Si ratio of the sample peaked in the first phase of the measurement (Fig. 15). This peak displays the lowering of Si concentration outwards the centre of sample, while Fe concentration rises. It can be assumed that sample has tiny iron coating. The concentrations of Ru^{101}, Rh^{103}, Pd^{105}, Os^{189}, Ir^{193}, and Pt^{195} were equivalent to the background or below the detection level.

5. Discussion

This research aimed to find, describe and hint for the origin of inorganic component of peat in Meenikunno bog. During the analysis, two samples were marked for their unusual morphology and optical/chemical properties.

Sample Meen_P2_3.6-3.7 is assumed to be a volcanic tephra shard. It has sharp edges and conchoidal fracture that is typical for volcanic glasses or minerals with high % of Si. Sample`s dimensions are less than 2 mm, thus can be classified as volcanic ash (Rose & Durant, 2009). Volcanic ash can travel hundreds to thousands of kilometres downwind from a volcano depending on wind speed, volume of ash erupted, and height of the eruption column. The size of ash particles that fall to the ground generally decreases exponentially with increasing distance from a volcano (Johnston, 1997).

As Estonia is a part of tectonically stable East-European craton, it is important to realize its distance from the nearest volcanoes, and the mechanisms behind eruptions. Wind and

eruption style are the two major controls on the dispersal of ash from an erupting volcano (Cas and Wright, 1987). Explosive eruption triggers voluminous plume of tephra. It is typical for felsic magmas, whereas basalt magmas usually generate very little ash.

Minerals within volcanic ash are primarily derived from the magma. Volcanic glass is relatively high in Si, but low in non-silica elements (especially Mg and Fe). Two spectral data of sample Meen_P2_3.6-3.7 were recalculated to oxides, so that the average wt% of SiO_2 was ca 79. This value could correspond to the rhyolite magma according to the alkali-silica (TAS) diagram. As it is a suspiciously high number, the wt % from lower SiO_2 concentration (61) was used. The alkali component (Na_2O+K_2O) comprised 8.6 wt %. The TAS diagram on Figure 16 illustrates the ratio between these components, and suggests a trachyte/andesite – trachyte type of magma. This supports the likelihood of ash plume formation.

Nevertheless, relatively large size of the sample (~ 1 mm) and long travel distances do not favour its volcanic origin.

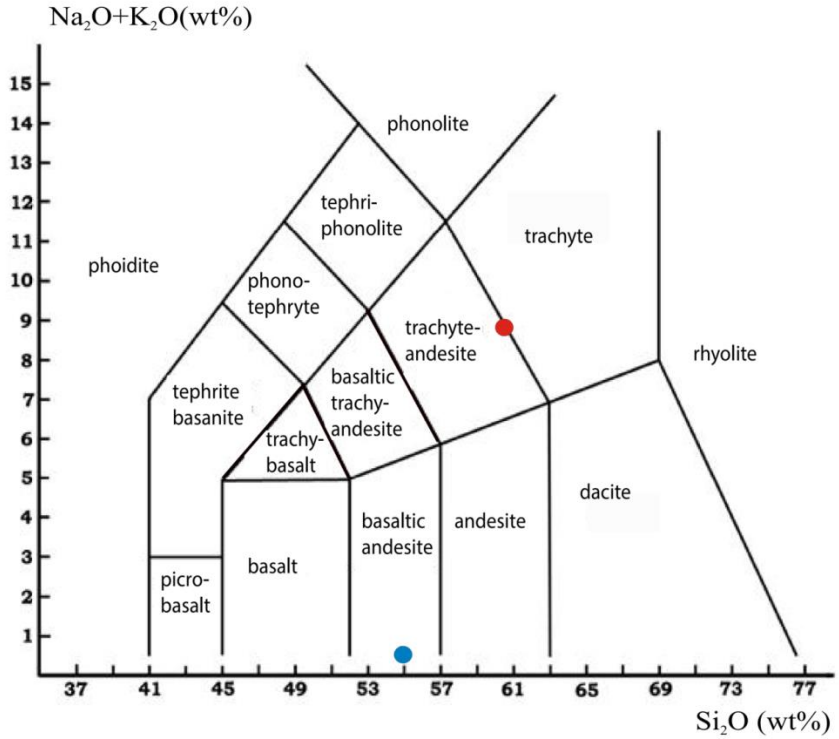

Figure 16. TAS diagram explaining different magma types in terms of their alkali-silica ratio. Red dot indicates a suggested magma composition for sample Meen_P2_3.6-3.7, whereas the blue one shows the position of sample Meen_P3_5.5-5.6.

Aero-dynamical shape of Meen_P3_5.5-5.6 implies sample`s airborne origin. Theoretically, it could also originate from volcanic activity. Based on SEM-EDS results, ca 55 wt % of SiO_2

and 0.7 wt % for Na_2O+K_2O were plotted on Figure 16 as well. However, it seems unlikely that basaltic-andesite magma may be associated with a higly explosive eruption.

Meen_P3_5.5-5.6 may be an example of impact spherule. Its chemical composition is relatively low in Si, high in Al and very low in Na. It correlates with Al-rich glassy spherules reported by Claeys & Casier in 1994, and spherules from Piila bog (Appendix 3) reported by E. Perle in 2014. Similar composition is also reported by Niyogi et al. (2011); however, the author warns that the shape, size, surface features, and chemistry of spherules are not diagnostic of impact cratering process. So it is hard to distinguish microtektites and impact spherules from the coal fly-ash spherules produced from natural fires and thermal power plants (Appendix 4).

The platinum-group elements (PGEs) are probably the most valuable elements for impact ejecta characterization. The PGEs along with siderophile elements, such as Ni and Co, occur at significantly higher concentrations in meteorites than in average crust. Distinctly higher siderophile elements content in impact melts, compared to target rock abundances, can be indicative of the presence of a chondritic or an iron projectile. Achondritic projectiles are much more difficult to discern (Koeberl et al., 2012).

IPC-MS analysis of Meen_P3_5.5-5.6 did not show the presence of PGEs, and Co-Ni values were miserable. Though, the measurement helped to indicate iron coating on the sample`s surface, which may had formed due to the leaching environment of peat. Similarly, E. Perle detected high iron concentration on spherule`s surface in 2014 (Appendix 5). It was done by SEM analysis that measured the brightest spot on one spherule. All spherules had elliptical shape, smooth darker surfaces with bright, thin striations on it. Basically, the SEM images from Perle (2014) resemble the sample of current research.

Raukas et al. (2001) studied Meenikunno peat, and found one layer with spherules that are up to some millimetres in size at the deph of 5.70 m. He also reported that they consist mainly of silica and calcium, with an admixture of iron, nickel, and several other elements. Even though this layer is only 10 cm below the one with sample Meen_P3_5.6-5.7, the appearance and chemistry of spherules is different. To compare the findings of current study with the previous one, former findings were also observed under the light microscope, photographed, and selected for SEM-EDS analysis.

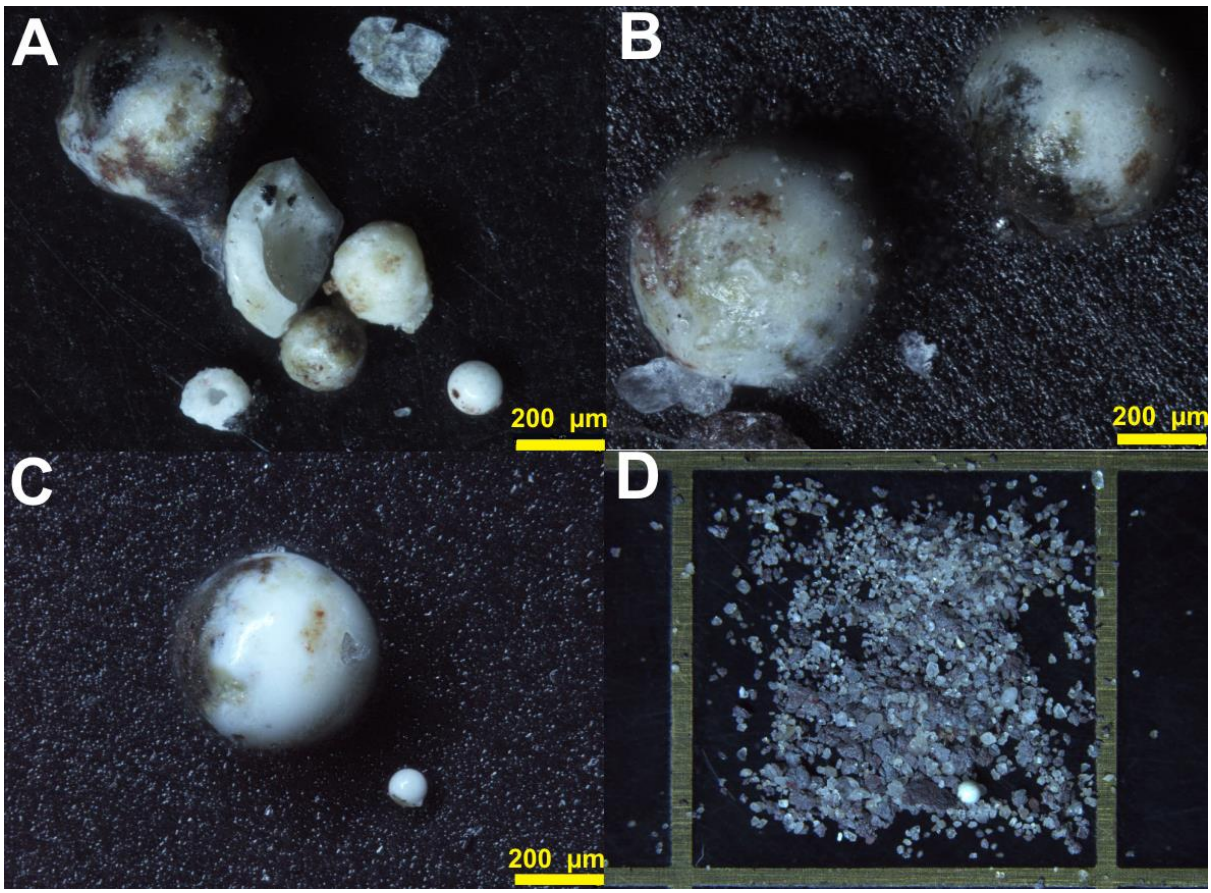

Figure 16. Glassy spherules from Mrs. Reet Tiirmaa collection. (A) Samples at the depth of 5.2-5.3 m. (B) Samples at the depth of 6.0-6.2 m. (C) Samples at the depth of 5.6-5.7 m. (D) Unsorted samples from the depth of 5.6-5.7 m. The square of 1 x 1 cm is for a scale.

The samples that resembled spherules were detected at the depths of 5.2-5.3, 6.0-6.2, and 5.6-5.7 (Fig. 16). The latter samples were collected from the all material of that depth by the author of this paper. The findings are whitish with yellow, brown, black inclusions, and have either rough surface with signs of melting or smooth and glossy one. The spherules have well-rounded, spherical shape, and the size range is variable: 100-550 µm.

SEM analysis of the samples indicated that generally Si and Ti are the most abundant elements, following by Ca/K, then by Na/Al/Fe, and then by S/P/Mg (Fig. 17-19). Although, the co-existence of Si and Ti in such amounts is unlikely (Kalle Kirsimäe per. com.). As titanium is paramagnetic, and iron concentration is relatively low, then these spherules cannot be classified as magnetic. Although, at the depth of 5.2-5.3 the concentration of Fe surpassed Si in one sample, and in the other Ni was detected.

Initial description by Raukas et al. (2001) about the size, appearance, and chemistry of the spherules hardly matches the observations done during this overview of Mrs Tiirmaa collection. Unclear is the presence of actually three depths of peat containing spherules, while

the initially stated depth of 5.70 m contains so few samples. This should mean either three separate events or extensive but very unlikely downward transportation of the inorganic material. Moreover, the appearance of these findings is similar to the ones from Piila mire (Appendix 6).

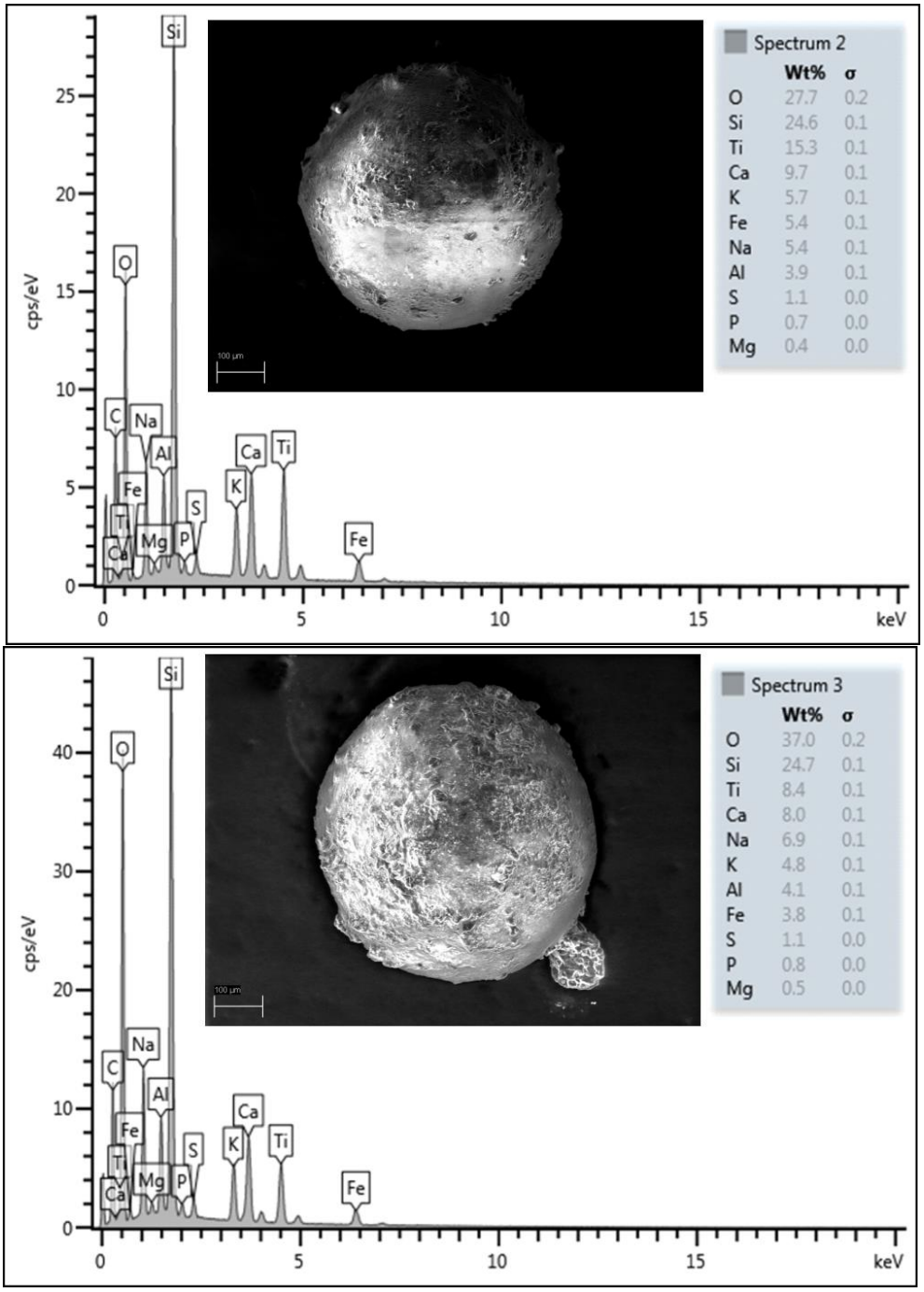

Figure 17. Spectral analysis and SEM image of two samples from Mrs. Reet Tiirmaa collection at the depth of 6.0-6.2 m.

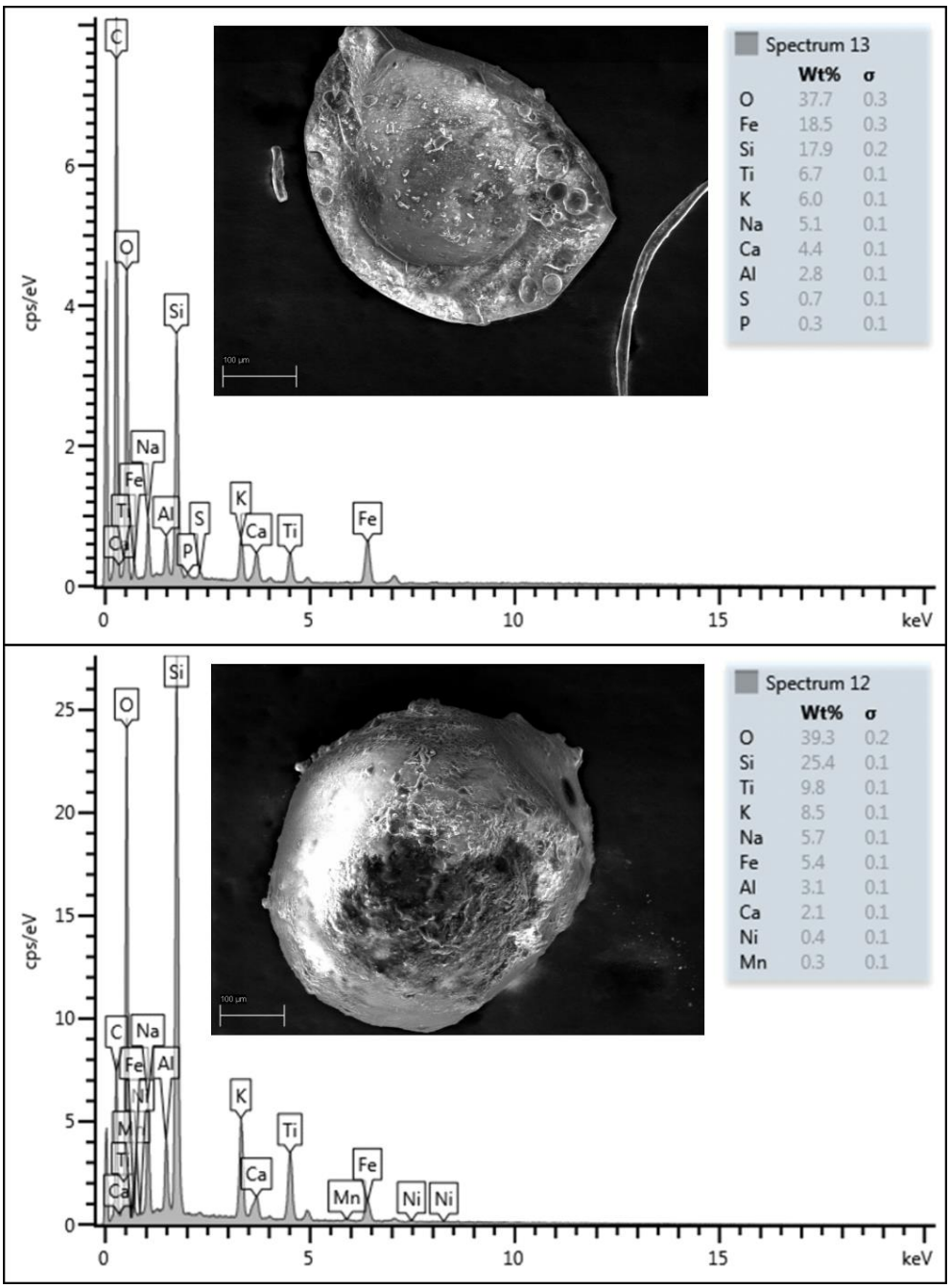

Figure 18. Spectral analysis and SEM image of two samples from Mrs. Reet Tiirmaa collection at the depth of 5.2-5.3 m.

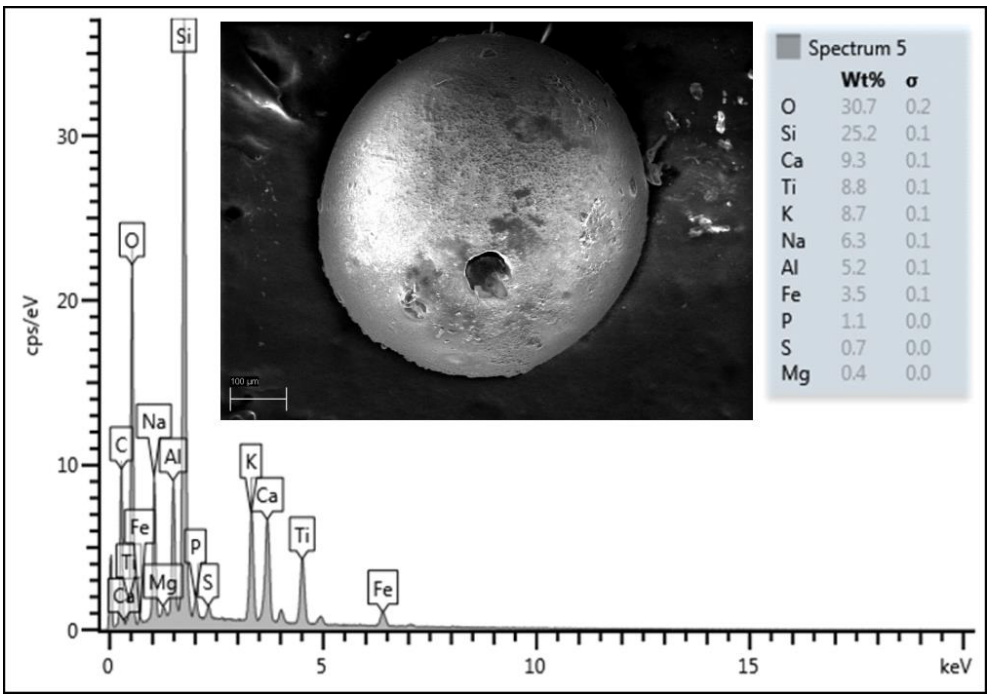

Figure 19. Spectral analysis and SEM image of the sample from Mrs. Reet Tiirmaa collection at the depth of 5.6-5.7 m.

6. Summary

Peatlands are great source for preservation of the volatile material that settles down on its surface. Later, this material is studied to determine its origin, and used as a stratigraphic marker tool. Raukas et.al. (2001) reported on presence of impact spherules in peat of Meenikunno bog.

The main purpose of current research was to conduct a GPR and peat coring study of Meenikunno bog in order to find and describe inorganic stratigraphic markers. The additional methods of magnetic susceptibility, LOI, light/optical microscopy, SEM-EDS and ICP-MS were applied.

GPR reflections showed the boundary between the peat and mineral deposit, although in some places the EM wave was disappearing. The maximum thickness of peat was identified as 7.92 m, and that is 0.82 m more compared to the previous study of Salo et al., 1985. The areas of high peat depth values form a NE-SW trending furrow. Peat description revealed several coal layers that overlapped distinct radar reflections.

The use of peat burning and light microscopy helped to discover 21 locations and 26 grains in the main peat cores Meen-P1, 2, and 3. Peat core Meen-P4-2 had 14 locations, and much more grains than Meen-P1, 2, and 3 altogether. The number of findings, as well as ash

content, and χ increase slightly downwards the peat cores. No spherule layers or their local concentration were identified by GPR and χ methods.

The majority of the grains were defined as sand particles, without closer study of their origin. However, two of the samples from Meen_P2_3.6-3.7 and Meen_P3_5.5-5.6 were carefully analysed in terms of their optical/chemical properties. Both of them showed clear distinction under the cross-polarized light revealing their glassy, amorphous structure.

In 2006 (Hang et. al.) first tephra layers were found in Estonian bogs. Sample Meen_P2_3.6-3.7 looks like glassy tephra shard. It is flat, angular, has interesting surface morphology, and one of its parts has conchoidal fracture (like in obsidian). These, along with sample`s chemistry support the theory of sample`s volcanic origin. Nevertheless, the size of the sample and its ability to travel long distances is doubtful.

Sample Meen_P3_5.5-5.6 is the only one from all findings that has an elongated, spheroidal shape, contains internal air bubbles, and resembles impact spherule. Its ICP-MS analysis showed no PGEs and almost no siderophile elements, which are known to be trace indicators of a chondritic or an iron projectile (Koeberl et al., 2012). The chemistry of the sample is similar to a recent study of spherules from Piila mire (Perle, 2014). Unlike SEM-EDS, ICP-MS method was more precise, and revealed iron coating on Meen_P3_5.5-5.6.

The comparison material from Mrs Reet Tiirmaa collection contained impact spherule-like samples that were detected at the depths of 5.2-5.3, 6.0-6.2, and 5.6-5.7 m. Unlike sample Meen_P3_5.5-5.6 (colourless), these findings are whitish with yellow, brown, and black inclusions. Tiirmaa spherules are also richer in variety of chemical elements.

The results of this paper confirm that there was a need for a more detailed study of Meenikunno inorganic component. This study comprised many different methods that were very helpful, but also rather time-consuming. The number of spherules and their location levels does not provide a clear answer whether there is a connection to Ilumetsa structures, and if they are of impact origin. However, more research can be done to increase the amount of spherule-like findings from Meenikunno, and to access their chemical properties.

7. Acknowledgements

I would like to thank various people for their contribution to this master thesis.

First, I want to thank Grisha and Karin for their help on a field work. Also, special thanks to Marko Kohv for his deep knowledge in peat properties.

Second, I really appreciate the advices received from Tiit Hang, Juho Kirs, and especially Kalle Kirsimäe for his valuable and constructive suggestions. Assistance from Peeter, Päärn, Giuseppe and Tõnu Meidla provided on performing laboratory work, SEM-EDS, and ICP-MS is greatly appreciated. Thanks to Argo Jõeleht, I have very valuable PC software and memorable talks.

I would like to express my very great appreciation to all the UT teachers that contributed their knowledge and skills for my learning process. Also, I extend my thanks to my course mates for their support and ability to have fun together.

I am particularly grateful for Mrs. Reet Tiirmaa for her previous work in the same research field, as well as for enjoyable meeting, and also for sharing her valuable knowledge and the collection of samples.

And last, the most important. A very special thank I address to my supervisor, Jüri Plado. He was the only person who readily agreed to cooperate and offered a couple of topics for a research. Our partnership started in August 2014, when we survived the warmest days of Estonian summer in Meenikunno bog. The cooperation evolved day by day through the sharing of his knowledge and skills. I would not have learned so much, if there was no Msc thesis and Jüri. He is very helpful and open-minded person with a good sense of humour. I would definitely suggest him as a supervisor to anyone.

8. References

Aaloe, A., 1960. Ilumetsa craters in Estonian SSR (in Russian). *Meteoritika* **18**, 26-31.

Dypvik, H., Plado, J., and Heinberg, C., 2008. Impact structures and events - A Nordic perspective. *Episodes* **31,** 107–114.

Cas, R.A.F., and Wright, J.V., 1988. Volcanic Successions: Modern and Ancient. Chapman & Hall, London, 528 pp.

Claeys, P. and Casier, J.G., 1994. Microtektite-like impact glass associated with the Frasnian-Famennian boundary mass extinction. *Earth Planetary Science Letters* **122,** 303–315.

Clymo, R. S., F. Oldfield, P. G. Appleby, G. W. Pearson, P. Ratnessar, and N. Richardson, 1990. A record of atmospheric deposition in a rain-dependent peatland. *Philosophical Transactions of the Royal Society of London* B **327**, 331–338.

Conyers, L.B., 2006. Ground-Penetrating Radar. In J.K. Johnson (ed.), *Remote Sensing Archaeology: An Explicitly North American Perspective*, University of Alabama Press, Tuscaloosa, 131–159.

Davis, J.L. and Annan, A.P. 1989. Ground-penetrating radar for high-resolution mapping of soil and rock stratigraphy. *Geophysical Prospecting* **37**, 531-551.

Ernston, K., Hiltl, M., and Neumair, A., 2014. Microtektite-like glasses from the Northern Calcareous Alps (Southeast Germany): evidence of a proximal impact ejecta. 45th Lunar and Planetary Science Conference, 1-2 pp.

French B.M. and Koeberl C., 2010. The convincing identification of terrestrial meteorite impact structures: What works, what doesn't, and why. *Earth-Science Reviews* **98**, 123-170.

Glass B.P. and Burns, C.A., 1988. Microkrystites: a new term for impact-produced glassy spherules containing primary crystallites. *Lunar and Planetary Science Conference* **18**, 455–458.

Glass B.P., 1990. Tektites and microtektites: key facts and inferences. *Tectonophysics* **171**, 393–404.

Glass, B.P. and Koeberl, C., 1999. Ocean Drilling Project Hole 689B spherules and upper Eocene microtektite and clinopyroxene-bearing spherule strewn fields. *Meteoritics and Planetary Science* **34**, 197-208.

Goldstein, J., 2003. Scanning Electron Microscopy and X-ray Microanalysis: Third Edition. *Springer US*, 689 pp.

Hang, T., Wastegård, S., Veski, S. and Heinsalu, A., 2006. First discovery of cryptotephra in Holocene peat deposits of Estonia, eastern Baltic. *Boreas* **35,** 644–649.

Hortolà, P., 2005. SEM Examination of Human Erythrocytes in Uncoated Bloodstains on Stone: Use of Conventional as Environmental-like SEM in a Soft Biological Tissue (and Hard Inorganic Material). *Journal of Microscopy* **218,** 94–103.

Ilomets, M. 1994. Turba juurdekasvust Eestis. *Eesti Geograafia Seltsi aastaraamat*, 26. kd. Teaduste Akadeemia Kirjastus, Tallinn, 13-18.

Johnston, D.M., 1997. Physical and social impacts of past and future volcanic eruptions in New Zealand, Unpublished Ph.D. thesis, University of Canterbury, Christchurch, 288 pp.

Kink, H., Andresmaa, E. ja Orru, M., 1998, Eesti soode hüdrogeoökoloogia, Teaduste Akadeemia Kirjastus, AS Pakett, Tallinn, 7-26.

Kink, H., Pirrus E. ja Metslang T., 1996. Meenikunno sookaitseala (The Meenikunno Mire Reserve) (in Estonian). In *Eesti Kaitsealad-Geoloogia ja vesi* (eds. A. Raukas and T. Kaasik), pp. 122-130. Teaduste Akadeemia Kirjastus, Tallinn, Estonia.

Koeberl, C., Claeys, P., Hecht, L. and McDonald, I., 2012. Geochemistry of impactites. *Elements* **8**, 37-42.

Marini, F. and Raukas, A., 2009. Lechatelierite-bearing microspherules from semicoke hill (Kiviõli, Estonia): Contribution to the contamination problem of natural microtektites. *Oil Shale* **26**, 415–423.

Masing, V., Aaviksoo K. and Kadarik H., 1997. Aerial views and close-up pictures of 30 Estonian mires. *The first book on telmatography*. Tallinn, 96 pp.

Moora, T., Raukas, A. and Stankowski, W.T.J., 2012. Dating of the Reo site (island of Saaremaa, Estonia) with silicate and iron microspherules points to an exact age of the fall of the Kaali meteorite, *Geochronometria* **39**, 262-267.

Niyogi, A., Pati, J.K., Patel, S.C., Panda, D. and Patil, S.K., 2011. Anthropogenic and impact spherules: Morphological similarity and chemical distinction - a case study from India and its implications. *Journal of Earth System Science* **120**, 1043–1054.

Perle, E., 2014. Turbaläbilõigete dateerimisvõimalused lenduvate osiste abil: Teici ja Piila raba näitel. Unpublished master's thesis. Tallinn, TTÜ, 66 pp.

Radar Systems, Inc. 2005. *Prism 2 Software Package. User`s Manual*. Riga, 45 pp.

Raukas, A, Pirrus, R, Rajamäe, R. and Tiirmaa, R., 1995. On the age of meteorite craters at Kaali (Saaremaa Island, Estonia). Proceedings of the Estonian Academy of Sciences, *Geology* **44**, 177–183.

Raukas, A., 1997. An attempt to use microimpactites in establishing the age of impact events on the example of the Kaali crater field (Estonia). *Sphaerula* **1**, 32–41.

Raukas A., 2000a. Investigation of impact spherules – a new promising method for the correlation of Quaternary deposits. *Quaternary International* **68** (71), 241-252.

Raukas A., 2000b. Study of meteoritic matter for precise regional stratigraphy. *Geologos* **5**, 77-86.

Raukas, A., Tiirmaa, R., Kaup, E. and Kimmel, K., 2001. The age of the Ilumetsa meteorite craters in southeast Estonia. *Meteoritics & Planetary Science*, **36**, 1507-1514.

Raukas, A. and Stankowski, W., 2011. On the age of the Kaali craters, Island of Saaremaa, Estonia. *Baltica* **24**, 37-44.

Rose, W.I. and Durant, A.J., 2009. Fine ash content of explosive eruptions. *Journal of Volcanology and Geothermal Research*, **186** (1-2), 32–39.

Salo, V., Võsa A. ja Kallas, R., 1985. Põlva rajooni Meenikonna turbamaardla detailse uuringu aruanne. ENSV Geoloogia Valitsus, Keila Geoloogiaekseditsioon, 67 pp.

Santisteban, J.I., Mediavilla, R., Lopez-Pamo, E., Dabrio, C.J., Zapata, M.B.R., Garcia, M.J.G., Castano, S. and Martinez-Alfaro, P.E., 2004. Loss on ignition: a qualitative or quantitative method for organic matter and carbonate mineral content in sediments? *Journal of Paleolimnology* **32**, 287–299.

Simonson, B.M., 2003. Petrographic criteria for recognizing certain types of impact spherules in well-preserved Precambrian successions; Rubey Colloquim paper; *Astrobiology* **3(1)** 49–65.

Simonson, B.M. and Glass, B.P., 2004. Spherule Layers—Records of Ancient Impacts. *Annual Review of Earth and Planetary Sciences* **32,** 329–361.

Stankowski, W.T.J., Raukas, A., Bluszcz, A. and Fedorowicz, S., 2007. Luminescence Dating of the Morasko (Poland), Kaali, Ilumetsa and Tsõõrikmäe (Estonia) Meteorite Craters. *Geochronometria*, **28,** 25–29.

Theimer, B.D., Nobes, D.C. and Warner, B.G., 1994. A study of the geoelectrical properties of peatlands and their influence on ground-penetrating radar surveying, *Geophysical Prospecting*, **42**, 179-209.

Veski, S., Heinsalu, A., Kirsimäe, K., Poska, A. and Saarse, L., 2001. Ecological catastrophe in connection with the impact of the Kaali meteorite about 800-400 B.C. on the island of Saaremaa, Estonia. *Meteoritics & Planetary Science* **36,** 1367–1375.

9. Kokkuvõte

Meenikunno raba turba anorgaaniliste osakeste uurimine georadari ja puurimiste andmetel

Jekaterina Nezdoli

Rabad on väga hea keskkond lenduva materjali säilimiseks. Turvast sageli kasutatakse, et uurida Kvaternaari stratigraafilisi sündmusi. Raukas et. al. (2001) leidis Meenikunno raba turbast sfääruli kihi sügavusel 5.7 m ja seostas seda Ilumetsa struktuuridega, aga tema leidud ei olnud piisavalt dokumenteeritud. Seega, tekkis vajadus uue uuringu jaoks. Selle uurimustöö põhieesmärgiks oli uurida Meenikunno raba turvast georadari ja puurimiste andmetel, et leida ja kirjeldada anorgaanilisi osakesi. Lisaks kasutati järgnevaid meetodeid: GRP, χ, SEM-EDS ja ICP-MS.

Elektromagnetlaine (EM) peegeldused näitasid turba ja mineraalpinnase vahelise piiri. Kuigi teatud sügavates kohtades EM laine signal kadus. Turba maksimaalseks paksuseks saadi 7.92 m, mis on 0.82 m rohkem, kui eelmisel Meenikunno raba uuringul (Salo et al., 1985). Turba sügavuste kaart näitas lode-kagu suunalist vaagumust uurimisala keskel. Turba läbilõigete kirjelduste käigus määrati põlengukihtide tasemeid. Need tasemed korreleeruvad radari väljapaistvate peegeldustega.

Turba põletamine ja valgusmikroskoobi kasutus aitas tuvastada 21 leidude taste ja 26 tera põhi puurakudes Meen-P1, 2, and 3. Puuraugus Meen-P4-2 määrati 14 taset ja palju rohkem teri, kui Meen-P1, 2 ja 3 kokku. Terade arv, tuhasus ja χ väärtused näitavad kergelt tõusvat trendi puuraukude sügavuste suhtes. Sfäärulite kogust või kihti GRP ja χ meetoditega pole tuvastatud.

Valdav enamus teradest klassifetseeriti liivaks, aga teri tasemetest Meen_P2_3.6-3.7 ja Meen_P3_5.5-5.6 analüüsiti põhjalikumalt. Mõlemad terad näitasid selget kustumist ristniikolites, paljastades nende klaasjat, amorfset struktuuri. Tera Meen_P2_3.6-3.7 on lapik, nurgaline ja meenutab tefra osakest. Selle pinnal esineb karpjas murre, mis on omane ka vulkaanilistele klaasidele. Tera morfoloogia ja keemia toetavad tema vulkaanilist päritolu, aga tera suurus paneb seda väidet kahtluse alla.

Tera Meen_P3_5.5-5.6 on ainuke leid kogu tööst, millel on väljavenitatud, sfääriline kuju ja esineb õhumulle. Need välised tunnused annavad julgust arvata, et tegu võib olla impaktsfääruliga. Selle ICP-MS ei näidanud PGE sisaldust, aga siderofiilsete elementide sisaldus oli tühine. ICP-MS meetod oli täpsem määramaks keemilisi elemente kui SEM-EDS. See näitas raua koorikut antud tera peal. Reet Tiirmaa koguse materjali väliskuju ja keemia ei ühtinud Meen_P3_5.5-5.6 teraga.

Selle töö käigus näidati erinevate meetodite kasutust turba anorgaanilise materjali uurimisel. Oma poolt leitud ning ka võrreldud sfäärulite tasemed, kogused ja keemia hetkel ei anna selget vastust, kas neid saab seostatada Ilumetsa kraatritega või mitte. Selleks on vaja uurida suuremat turba kogust ning teha edasisi analüüse.

10. Appendix

Appendix 1a. Description of peat core sections Meen-P1 and Meen-P2 (data are provided by Marko Kohv).

	Thickness (m)	Peat type	Decomposition rate	Comments
meen-P1	0-0.13	void (no peat)		
	0.13-0.20	eriophorum-sphagnum	1-2	
	0.20-0.57	eriophorum-sphagnum	3-5	
	0.57-1.49	eriophorum-sphagnum	3-5	
	1.49-1.85	eriophorum-sphagnum	4	dark brown; 1.50 - burned
	1.85-2.0	eriophorum-sphagnum+ shrub	2	dark brown
	2.0-2.29	eriophorum-sphagnum	1	
	2.29-3.5	eriophorum-sphagnum	2-7	2.33, 2.56, 2.96 - burned
	3.5-3.90	pinus	9	
	3.90-4.05	shrub-sphagnum + eriophorum	3	
	4.05-4.37	eriophorum-sphagnum + wood	6-7	
	4.37-4.60	eriophorum-sphagnum + shrub	2	
	4.60-4.77	eriophorum-sphagnum +wood	7	
	4.77-5.40	sphagnum-eriophorum	4	equisetum (?)
	5.40-5.70	equisetum-carex + eriophorum	1	menyanthes
	5.70-5.85	equisetum	4	black; thick
	5.85-5.92	transition		from peat to sand
	5.92-6.0	gyttja-sand	Lake sediments	fine-grained, + mica
meen-P2				
	0-0.1	void (no peat)		
	0.10-0.25	shrub-sphagnum	2-3	dark brown
	0.25-0.85	eriophorum-sphagnum	1	yellow-brown
	0.85-0.95	sphagnum	3	
	0.95-1.27	eriophorum-sphagnum	2	brown
	1.27-2.41	eriophorum-sphagnum	2	2.28, 2.85 - burned
	2.41-2.63	sphagnum-pinus + eriophorum	6	
	2.63-3.0	eriophorum-sphagnum	5-7	dark brown
	3.0-3.25	eriophorum-sphagnum	2	
	3.25-3.55	sphagnum-shrub-pinus	8	
	3.55-3.75	eriophorum-sphagnum + wood	5	dark brown
	3.75-4.0	eriophorum-pinus + wood	9	
	4.0-4.4	eriophorum-wood-sphagnum	7	
	4.4-4.65	equisetum-wood + eriophorum	5	
	4.65-4.85	equisetum-carex	1.5	fen
	4.85-4.95	equisetum + wood	3	thick, tough
	4.95-4.99	transition		from peat to sand
	4.99+	unsorted sand		beige; lake shore area (?)

Appendix 1b. Description of peat core sections Meen-P3 and Meen-P4-1 and 2 (data are provided by Marko Kohv).

	Thickness (m)	Peat type	Decomposition rate	Comments
meen-P3	0-0.35	void (no peat)		
	0.35-0.80	eriophorum-sphagnum	1-2	yellow-brown
	0.8-0.95	sphagnum-eriophorum	3-5	dark brown
	0.95-1.35	sphagnum	2	red-brown
	1.35-1.60	heather-sphagnum	2	yellow-brown
	1.60-1.75	eriophorum-sphagnum	2	dark brown
	1.75-2.0	sphagnum-pinus	4-8	dark brown
	2.0-2.55	eriophorum-sphagnum	2	brown; 2.34 - burned
	2.55-2.75	sphagnum	1.5	brown
	2.75-2.92	sphagnum-pinus	5	dark brown; big wood pieces inside
	2.92-3.48	heather-sphagnum	1.5	dark brown; 3.11 - burned
	3.48-3.88	heather-sphagnum-pinus	7	dark brown; 3.5 - burned (?)
	3.88-4.18	heather-eriophorum-sphagnum	3	dark broown
	4.18-4.88	sphagnum-eriophorum-pinus	3-6	dark brown; 4.50 (?), 4.70 - burned
	4.88-5.07	eriophorum-pinus	9	dark brown
	5.07-5.40	pinus-sphagnum-eriophorum	8	dark brown
	5.40-5.70	sphagnum-eriophorum-pinus	8	dark brown; thick
	5.70-6.0	pinus-eriophorum-sphagnum	5	dark brown
	6.0-6.30	eriophorum-sphagnum	3	yellow-brown; + wood
	6.30-6.50	carex-equisetum	2	yellow-brown; + wood; sedge mire stage
	6.50-6.78	eriophorum-carex + equisetum	1.5	yellow-brown; menyanthes; cranberry
	6.78-6.92	puidu-osja	6	black; fen stage
	6.92-7.0	transition to gyttja	9-10	with mineral particles
	7.0 +	silt-gyttja		sandy interlayers; mica; lake-origin
meen-P4-1				
	6.50-6.61	carex-equisetum	1-2	menyanthes
	6.61-6.68	equisetum	6	
	6.68-7.50	silt-fine sand		layered; 1 layer ~1-2 cm; + plant remains
meen-P4-2				
	5.0-5.65	pinus	8	sphagnum, heather, eriophorum
	5.65-6.15	wood	3-5	carex, sphagnum; broadleaf tree pieces
	6.15-6.57	carex	2	bryopsida, phragmites, equisetum, wood
	6.57-6.66	bryopsida-equisetum	4	
	6.66-7.0	silt-sand	lake origin	grey-beige; layered; plant remains; mica

Appendix 2a. SEM-EDS of the sample from Meen-P4_5.2-5.3 m.

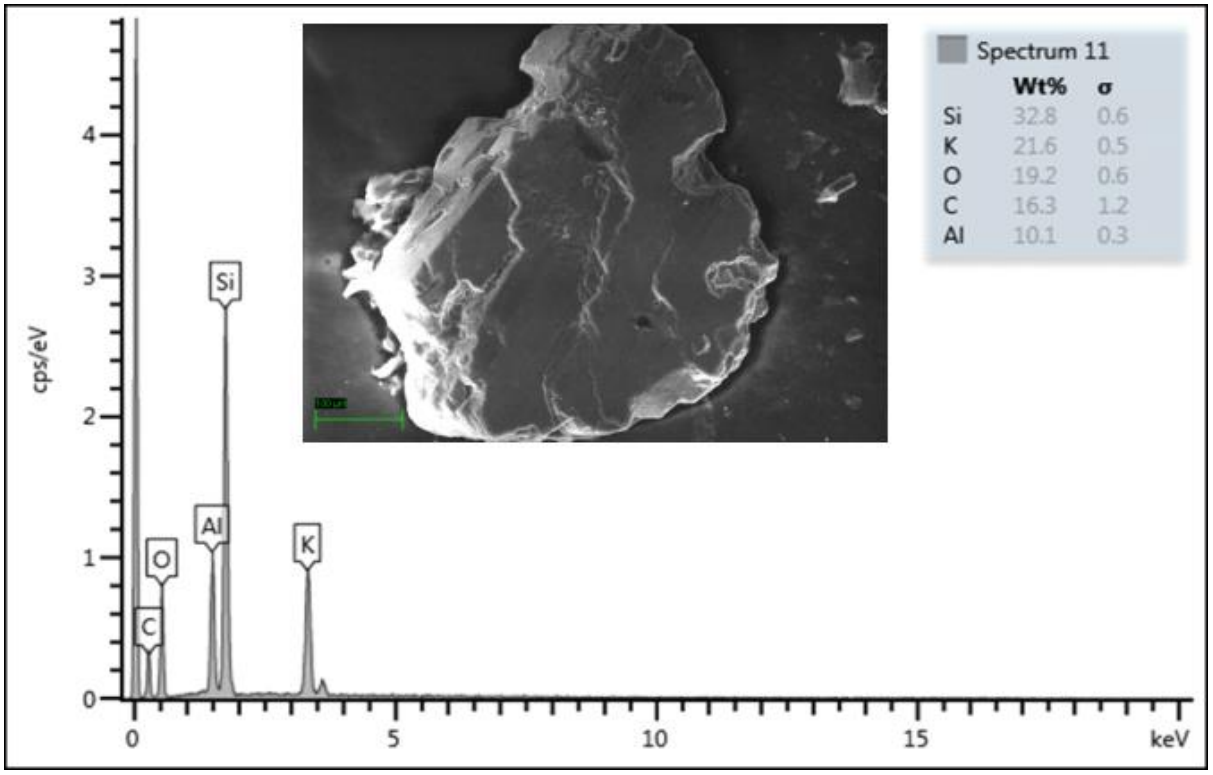

Appendix 2b. SEM-EDS of the sample from Meen-P4_5.6-5.7_1 m.

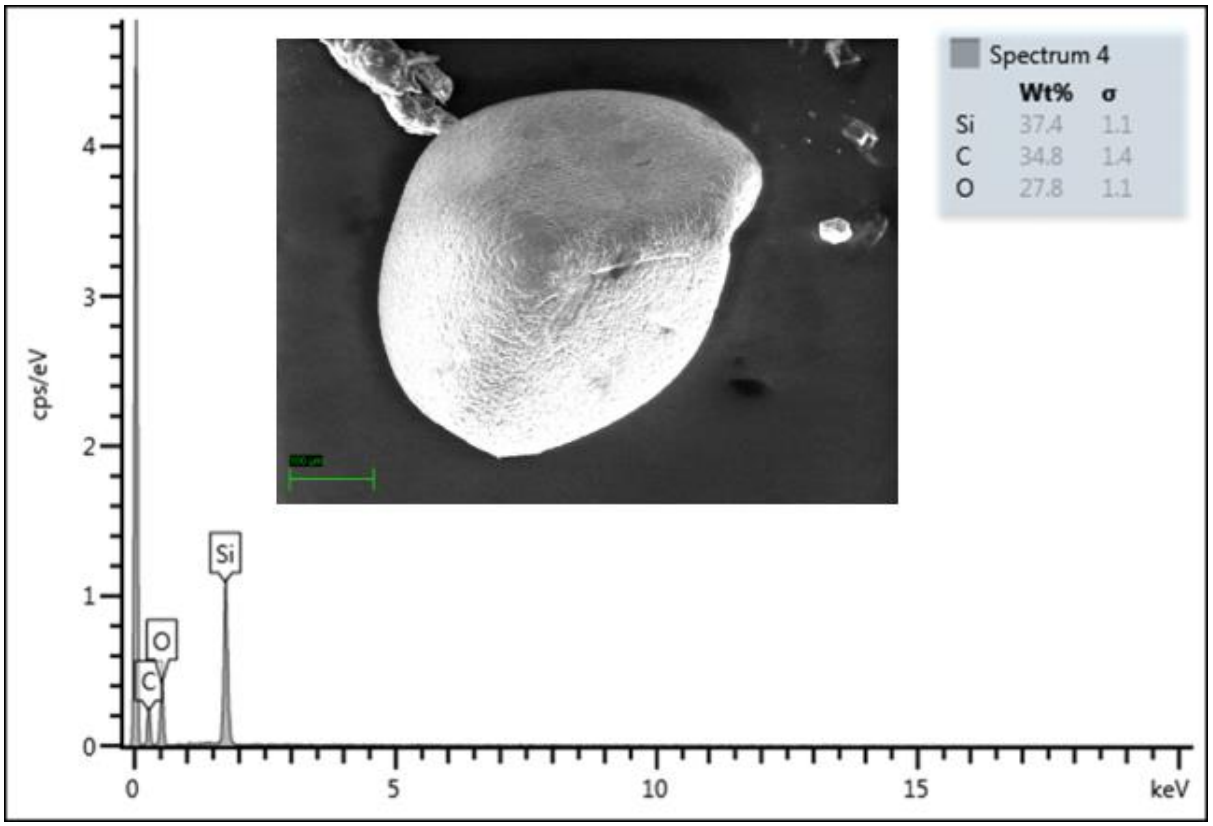

Appendix 2c. SEM-EDS of the sample from Meen-P4_5.6-5.7_2 m.

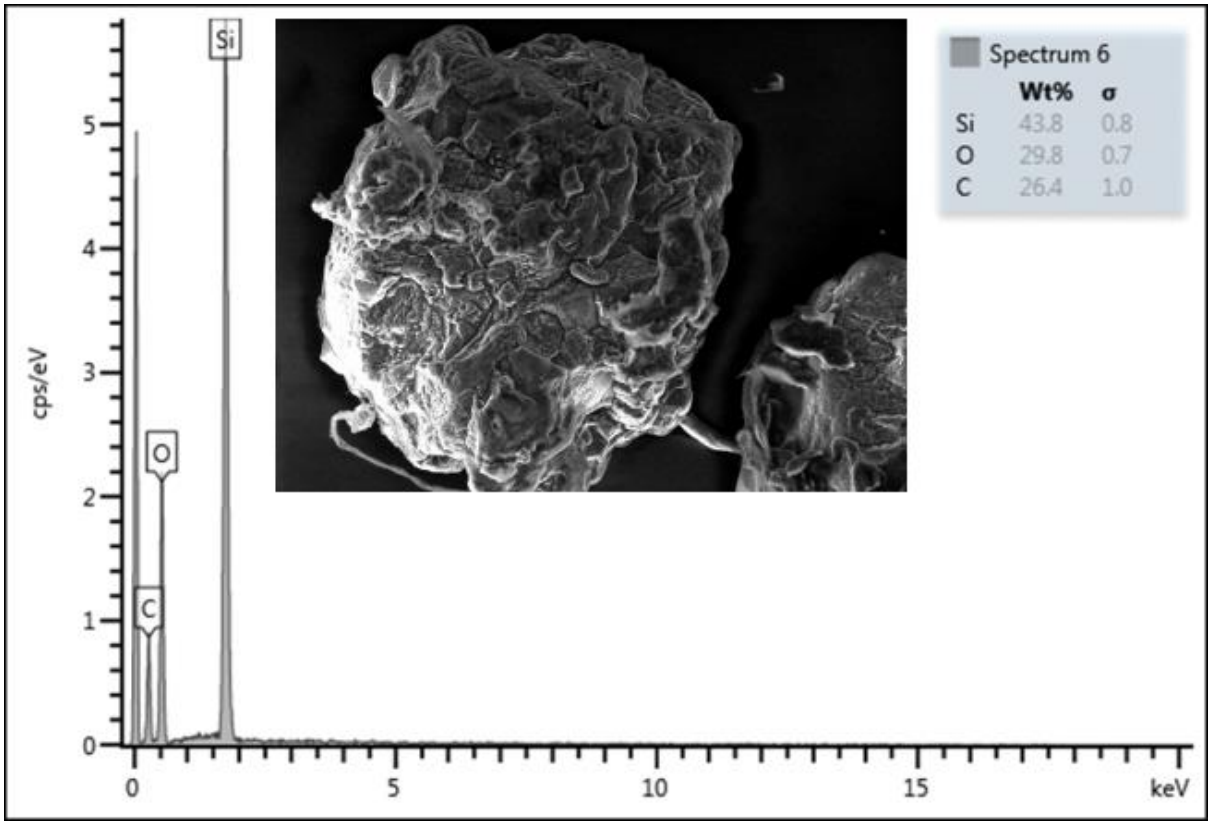

Appendix 2d. SEM-EDS of the sample from Meen-P4_6.0-6.1 m.

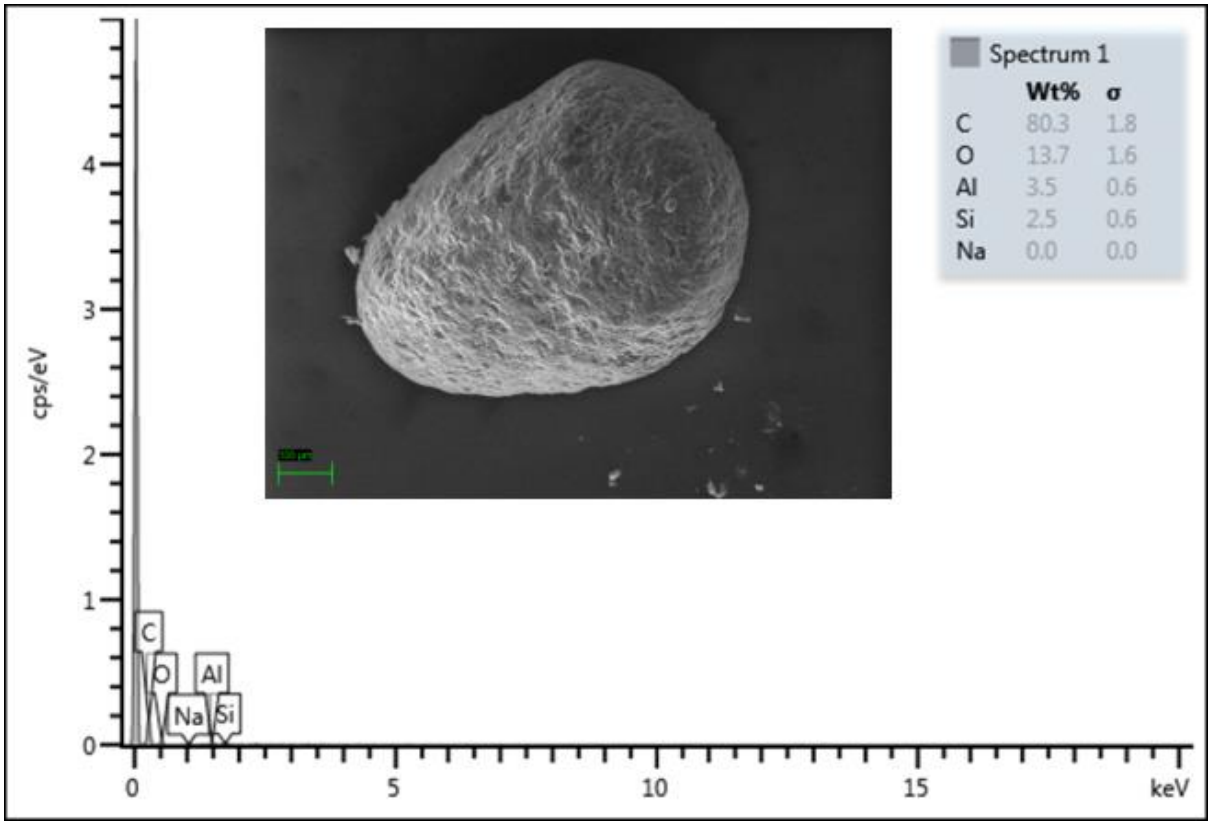

Appendix 3. A comparison between microtektites, impact - and anthropogenic spherules in the study by Niyogi et al., 2011.

Spherule type	Shape	Size	Colour	Chemical composition
Microtektites	Spherical, elongated, teardrop, discs or dumbbell, spindle, club-shaped, bun-shaped	<1 mm	Honey coloured, light yellow, yellowish green to opaque white	SiO_2: 56.26–75.74 (Avg. 68.59) Na_2O: 0.41–1.04 (Avg. 0.66) K_2O: 0.33–2.02 (Avg. 1.00) Al_2O_3: 10.63–21.12 (Avg. 15.33) MgO: 2.38–10.62 (Avg. 4.66) CaO: 2.06–4.14 (Avg. 3.24) FeO: 3.97–9.16 (Avg. 5.42) TiO_2: 0.56–1.07 (Avg. 0.84)
Impact spherule	Spherical, teardrop, cylinder, dumbbell and spindle	≈0.3−1 mm		SiO_2: 43.33–51.39 (Avg. 48.31) Al_2O_3: 11.76–15.23 (Avg. 13.67) Na_2O: 1.23–2.38 (Avg. 1.81) MgO: 4.95–8.93 (Avg. 6.84) K_2O: 0.19–0.78 (Avg. 0.32) CaO: 8.21–10.71 (Avg. 9.24) FeO: 11.96–16.89 (Avg. 15.27) TiO_2: 1.94–2.95 (Avg. 2.32) P_2O_5: 0.02–0.16 (Avg. 0.07)
Anthropogenic spherule (present study)	Spherical, elliptical, dumbbell, spindle, teardrop and cylinder	0.55–1.67 mm	Colourless to dark grey, opaque white, brown	SiO_2: 67.10–77.07(Avg. 72.09) Al_2O_3: 1.21–3.63 (Avg. 1.70) Na_2O: 0.19–6.79 (Avg. 2.31) MgO: 3.62–0.30 (Avg. 1.97) K_2O: 0.26–1.04 (Avg. 0.50) CaO: 5.01–10.16 (Avg. 7.57) TiO_2: 0.01–0.08 (Avg. 0.03) FeO^*: 0.07–0.40 (Avg. 0.21) P_2O_5: 0.09–0.17 (Avg. 0.13)

Appendix 4. The mean chemical composition of spherules in Piila mire (Perle, 2014).

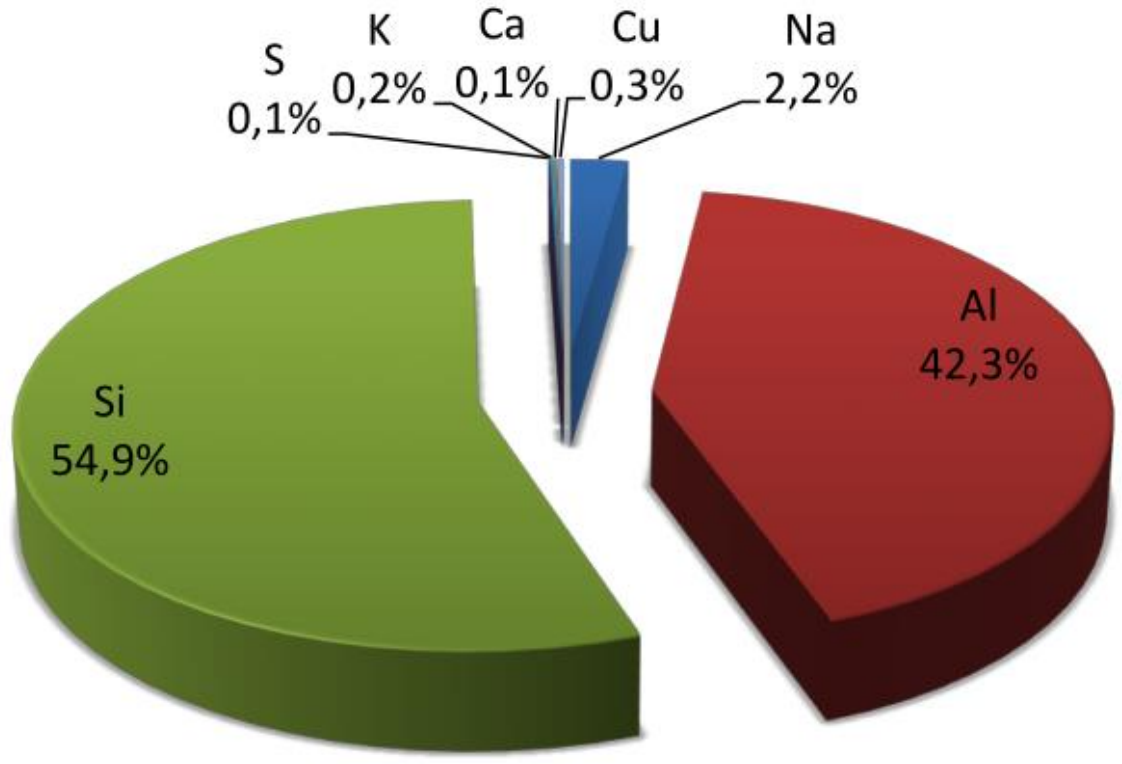

Appendix 5. Above is the chemical composition of the bright spot on the spherule nr. 2, and below is SEM image of it.

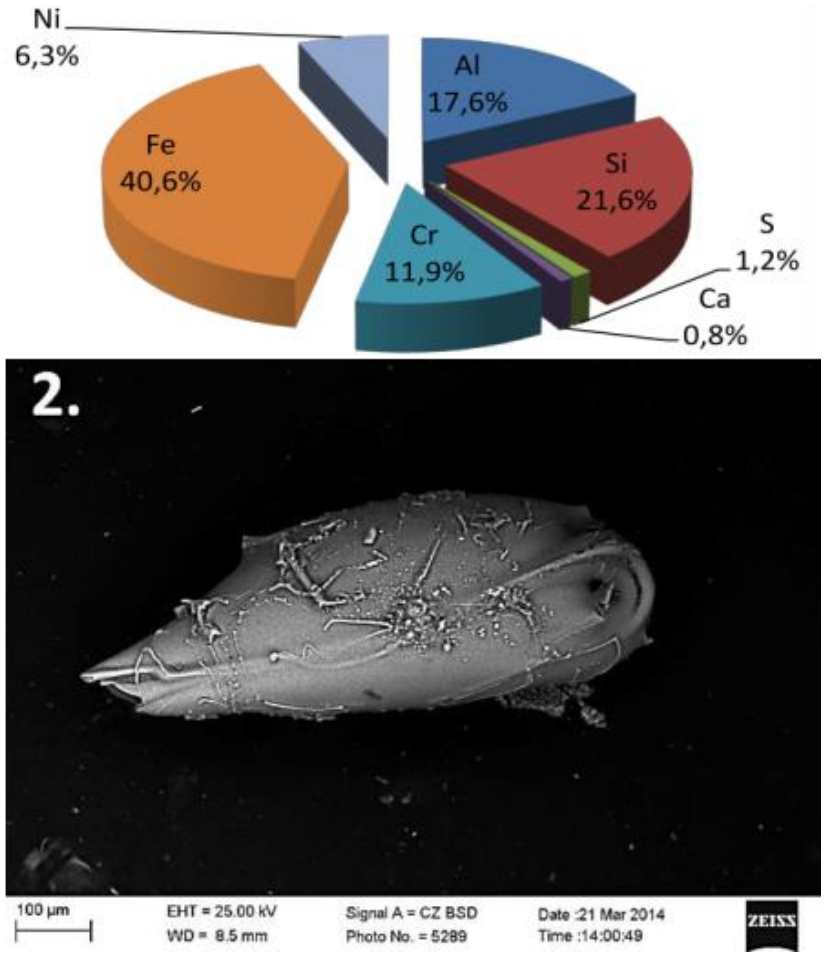

Appendix 6. Typical glassy spherules from the Piila Mire at a depth of 3.00 – 3.10 m accumulated during the Kaali impact (Marini & Raukas, 2009).

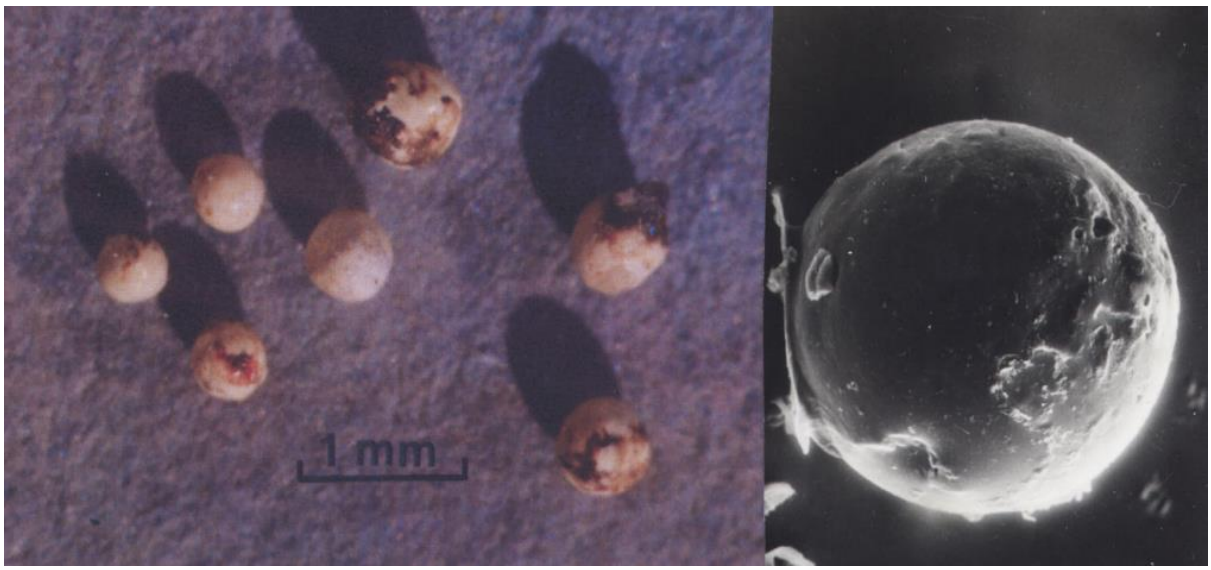

Non-exclusive licence to reproduce thesis and make thesis public

I, Jekaterina Nezdoli

1. herewith grant the University of Tartu a free permit (non-exclusive licence) to:

1.1. reproduce, for the purpose of preservation and making available to the public, including for addition to the DSpace digital archives until expiry of the term of validity of the copyright, and

1.2. make available to the public via the web environment of the University of Tartu, including via the DSpace digital archives until expiry of the term of validity of the copyright,

Study of inorganic component within the Meenikunno bog (SE Estonia) peat

supervised by Jüri Plado

2. I am aware of the fact that the author retains these rights.

3. I certify that granting the non-exclusive licence does not infringe the intellectual property rights or rights arising from the Personal Data Protection Act.

Tartu, **21.05.2015**